POLITECNICO DI TORINO
Repository ISTITUZIONALE

Injectable supramolecular hydrogels based on custom-made poly(ether urethane)s and -cyclodextrins as efficient delivery vehicles of curcumin

Original
Injectable supramolecular hydrogels based on custom-made poly(ether urethane)s and -cyclodextrins as efficient delivery vehicles of curcumin / Torchio, A., Cassino, C., Lavella, M., Gallina, A., Stefani, A., Boffito, M., Ciardelli, G.. - In: MATERIALS SCIENCE AND ENGINEERING. C, BIOMIMETIC MATERIALS, SENSORS AND SYSTEMS. - ISSN 0928-4931. - ELETTRONICO. - 127:(2021), pp. 1-19. [10.1016/j.msec.2021.112194]

Availability:
This version is available at: 11583/2904392 since: 2021-06-04T17:06:48Z

Publisher:
Elsevier

Published
DOI:10.1016/j.msec.2021.112194

Terms of use:

This article is made available under terms and conditions as specified in the corresponding bibliographic description in the repository

Publisher copyright
Elsevier postprint/Author's Accepted Manuscript

© 2021. This manuscript version is made available under the CC-BY-NC-ND 4.0 license
http://creativecommons.org/licenses/by-nc-nd/4.0/.The final authenticated version is available online at:
http://dx.doi.org/10.1016/j.msec.2021.112194

(Article begins on next page)

17 November 2026

This is an author version of the contribution published on:

Materials Science and Engineering: C

Volume 127, August 2021, 112194

doi: 10.1016/j.msec.2021.112194

The definitive version is available at:

https://www.sciencedirect.com/science/article/pii/S0928493121003337?dgcid=author#s0225

Injectable supramolecular hydrogels based on custom-made poly(ether urethane)s and α-cyclodextrins as efficient delivery vehicles of curcumin

Alessandro Torchio[a,b], *Claudio Cassino*[c], *Mario Lavella*[a,d], *Andrea Gallina*[c], *Alice Stefani*[a,e], *Monica Boffito*[a,#,*], *Gianluca Ciardelli*[a,#]

[a] Department of Mechanical and Aerospace Engineering, Politecnico di Torino, Corso Duca degli Abruzzi 24, 10129, Torino, Italy

[b] Department of Surgical Sciences, Università degli studi di Torino, Corso Dogliotti, 14, 10126, Torino, Italy.

[c] Department of Science and Technological Innovation, Università del Piemonte Orientale "A. Avogadro", Viale Teresa Michel 11, 15121, Alessandria, Italy.

[d] Department of Management, Information and Production Engineering (DIGIP), Università degli Studi di Bergamo, Viale G. Marconi, 5, 24044 Dalmine (BG) Italy

[e] Chemical and Biological Laboratory Safe S.r.l., Via di Mezzo 48, 41037, Mirandola (MO), Italy.

[#] These authors have contributed equally to the supervision of the first author

* Corresponding author

ABSTRACT

A strategy to enhance drug effectiveness while minimizing controversial effects consists in exploiting host-guest interactions. Moreover, these phenomena can induce the self-assembly of physical hydrogels as effective tools to treat various pathologies (e.g., chronic wounds or cancer). Here, two Poloxamers®/Pluronics® (P407/F127 and P188/F68) were utilized to synthesize various LEGO-like poly(ether urethane)s (PEUs) to develop a library of tunable and injectable supramolecular hydrogels for drug delivery. Three PEUs were synthesized by chain extending Poloxamer/Pluronic with 1,6-cyclohexanedimethanol or N-Boc serinol. Other two amino-functionalized and highly responsive polymers were obtained thorough Boc-group cleavage. For hydrogel design, the spontaneous self-assembly of the poly(ethylene oxide) domains of PEUs with α-cyclodextrins was exploited to form poly(pseudo)rotaxanes (PPRs). PPR-derived channel-like crystals were characterized by X-Ray powder diffraction, Infra-Red and Proton Nuclear Magnetic Resonance spectroscopies. Cytocompatible hydrogel formulations were designed at PEU concentrations between 1% and 5% w/v and α-cyclodextrin at 10% w/v. Supramolecular gels showed good mechanical performances (storage modulus up to 20 kPa) coupled with marked thixotropic and self-healing properties (mechanical recovery over 80% within 30 seconds

after cyclic rupture) as assessed through rheology. Hydrogels exhibited stability and high responsiveness in watery environment up to 5 days: the release of less stable components as suitable drug carriers was coupled with high swelling (doubling the content of fluids with respect to their dry mass) and shape retention. Curcumin was encapsulated into the hydrogels at high concentration (80 μg ml^{-1}) through its complexation with α-cyclodextrins and delivery tests showed controllable and progressive release profiles up to four days.

KEYWORDS: Supramolecular hydrogels; self-healing hydrogels; cyclodextrin-based host-guest complexes; thermo-sensitive polyurethanes; smart drug delivery

1. Introduction

Cyclodextrins (CDs) are cyclic molecules based on alpha 1-4 linked glucose monomers. The most common CDs are composed of 6, 7 and 8 glucose units and are classified as α-CD, β-CD, and γ-CD, respectively. Their conformation is characterized by an inner hydrophobic cavity and an outer hydrophilic wall, which size depends on the number of constituent glucose units. Because of their morphology, CDs can encapsulate a wide variety of different molecules, thus forming host-guest inclusion complexes.[1] For this peculiarity and thanks to their cost-effective industrial production,[2] CDs are widely used in various fields, such as in pharmaceutics,[3,4] food technology,[5] cosmetics,[6] and de-toxification systems.[7] Moreover, CDs can be chemically modified, thus opening the way to the possibility to produce poly-functional derivatives.[4,8] Nevertheless, even virgin CDs can find many applications in the biomedical field. In fact, CDs can encapsulate and transport drugs, as well as interact with many natural molecules present in biological environments, (e.g., cholesterol, vitamins, and other hydrophobic molecules).[9] It is noteworthy that CD interaction with any guest molecule is not driven by a specific recognition process, as in the case of enzymes and their substrates. Indeed, the only requirements for the formation of CD-based complexes are the dimensional match of CD cavity with the guest and the mutual hydrophobicity of the two components.[10,11] In the case of drug encapsulation, the resulting supramolecular assemblies could present many advantages respect to drug molecules as such: i) greater solubility in watery environments, ii) prolonged chemical stability, and iii) enhanced biological availability. In particular, the formation of supramolecular complexes between CDs and curcuminoids and the resulting pros of such assemblies have been deeply studied over the last decades. Curcumin is the most diffused constituent of *Curcuma longa* (i.e.,

a turmeric) and it has been applied in medicine from decades as anti-microbial,[15–17] antitumor,[18–20] anti-inflammatory and antioxidant[21,22] agent. Moreover, curcumin has been widely used in tissue engineering strategies as a remedy for skin wounds and bone healing due to its ability to stimulate the deposition of extra-cellular matrix while modulating the inflammatory response.[23] However, due to the highly hydrophobic nature of curcumin, its bioavailability is generally very low.[24] In this regard, a significant improvement in its therapeutic effects can be achieved through its encapsulation into smart polymeric nanocarriers for systemic or *in loco* delivery.[25–27] Other strategies consist in encapsulating curcumin directly into bulky supports, such as hydrogels[28] or scaffolds[29]. Recent approaches have also combined curcumin-loaded nanocarriers with hydrogels to develop formulations with an additional control over the payload release kinetics and improved curcumin bioavailability and *in vivo* stability[30–32]. As anticipated above, a relevant role in this scenario is also represented by the complexes that can be formed between curcumin and CDs. Thanks to their bigger cavity, β-CDs, γ-CDs and their derivatives are widely used to encapsulate curcumin mainly through inclusion complexes formation.[33–37] Nevertheless, even the smaller α-CDs can show a remarkable ability as solubilizing agents of curcumin through the formation of simple inclusion complexes or the occurrence of higher order self-assembly mechanisms based on the aggregation of smaller complexes.[38–40] It has also been demonstrated that α-CDs exert an effective protection on curcumin from degradation in alkaline milieu, enhancing its transport and absorption in biological environments with no significant toxic effects.[41]

In addition to the capability to form complexes with drug molecules, α-CDs are also widely used to develop supramolecular hydrogels, which can be defined as highly organized networks resulting from physical interactions. As a result of this feature, supramolecular hydrogels usually exhibit enhanced physical properties (i.e., stability, responsiveness to external environment, mechanical properties and also reversibility) compared to systems based on less ordered or chemically crosslinked networks.[42] In this scenario, one particular arrangement is based on the inclusion complexes that natural macrocycles and linear aliphatic polymers spontaneously form.[43,44] In fact, α-CDs have been exploited to form supramolecular hydrogels based on poly(pseudo)rotaxanes (PPRs). In detail, PPRs are linear complexes composed of threaded CDs along polymer chains.[10] The most well-known interaction consists in the formation of polymer-based inclusion complexes between poly(ethylene oxide) and α-CDs.[45,46] It has been demonstrated that these structures can further assemble into channel-like supramolecular crystals thus resulting in stable networks suitable for hydrogel formation.[47,48] The same supramolecular gelation process can be found in other recent works, in which poly(ethylene

oxide)- (PEO) and poly(propylene oxide)- (PPO) based block-copolymers (PEO-PPO-PEO or PPO-PEO-PPO, Pluronics®/Poloxamers® or their reverse form, respectively) have been investigated.[49,50] Generally, it has been hypothesized that the presence of hydrophobic domains could induce a stabilizing effect during the formation of the supramolecular PPR-based network.[50,51] For instance, the above-mentioned supramolecular systems were characterized by remarkable elastic moduli and high reversibility (i.e., self-healing) due to their physical and hierarchical nature. For all these properties, these supramolecular hydrogels have been widely applied for the delivery of different therapeutic agents, such as immunoglobulin G [52] and vancomycin[53]. Other examples in the literature report the design and characterization of supramolecular hydrogels based on different PEO-based co-polymers (e.g., polylactic acid[54,55], poly(ε-caprolactone)[56,57] or poly[(R)-3-hydroxybutyrate][58]). Hence, α-CDs hold huge promise in the biomedical field as both trigger for the formation of hydrogels with proper physico-chemical and biological properties and drug carriers enhancing the bioavailability and the effects of therapeutic agents. The development of new polymeric materials to formulate CD-based hydrogels with enhanced properties is relatively noteworthy nowadays, as recently and accurately discussed by Domiński *et al.*.[59] However, to the best of our knowledge, only very few examples in the literature report on PPR-based systems with both marked responsiveness and stability in contact with watery environments.[54,60] In fact, relatively high polymeric contents are usually required to reach good mechanical performances,[53,59,61] thus increasing the risk of local or systemic toxicity.[62] Starting from these premises, in this work the role of CDs was engineered for both hydrogel formation and drug encapsulation and new custom-made multiblock copolymers were investigated for hydrogel design. Indeed, we aimed to conjugate the therapeutic effects of curcumin with properly synthesized PEO-based poly(ether urethane)s (PEUs) for the design of versatile supramolecular hydrogels as delivery platforms with enhanced tunability, stability and mechanical response. In our previous study, PEO-based PEUs have shown the ability to form stable supramolecular hydrogels at low PEU concentrations (i.e., ranging between 1% and 5% w/v).[63] In this work, in order to further explore the final effects of PEU chemical composition as tuning feature on the resulting supramolecular hydrogel systems, Poloxamer® 407 (P407, 70% wt PEO, $\overline{M}_n$ 12600 Da) and Pluronic® F68 (F68, 80% wt PEO, $\overline{M}_n$ 8400 Da) were selected as macrodiols and pre-polymerized with 1,6-hexamethylene diisocyanate (HDI); then, two different chain extenders (1,4-cyclohexanedimethanol (CDM) and N-Boc serinol (NBoc)) were used to produce the final polymers. Furthermore, NBoc-containing PEUs were subjected to a Boc group cleavage reaction under acid conditions, leading to primary amine exposure along PEU backbone and the possibility to investigate the potential role exerted by pendant functionalities on

supramolecular hydrogel formation.[64,65] The formation of PPR-based supramolecular structures was first characterized through X-Ray Powder Diffraction (XRD), Attenuated Total Reflectance - Fourier Transformed Infra-red (ATR-FTIR) and Proton Nuclear Magnetic Resonance (^{1}H-NMR) Spectroscopies. Supramolecular hydrogels were then formulated in phosphate buffered saline (PBS, pH 7.4) at PEU concentrations from 1% to 5% w/v and α-CDs content at 10% w/v. The resulting gels were thoroughly characterized in terms of their physical properties in order to identify potential relationships between PEU chemical structure and the resulting supramolecular gel properties. Moreover, mechanical properties and self-healing ability were evaluated through a complete rheological characterization. Biological compatibility was tested according to ISO10993 standards using pure gel extracts. Finally, in order to prove the feasibility of the developed supramolecular hydrogels as real drug delivery platforms for the treatment of various pathologies (e.g., cancer, infections or acute inflammation), the encapsulation of curcumin at high concentration (i.e., 80 μg ml^{-1}, approx. 130-fold higher than curcumin solubility in water[41]) was performed exploiting the presence of both PEU-based micelles and α-CDs. Finally, release tests were conducted to evaluate curcumin release profiles in biological-like environments (i.e., at pH 7.4 and 37 °C).

2. Materials and Methods

2.1 Materials

Poloxamer® 407 (P407, $\bar{M}_n$ 12600 Da) and Pluronic® F68 (F68, $\bar{M}_n$ 8400 Da), HDI (168.2 Da), CDM (144.2 Da), NBoc (191.2 Da), dibutyltin dilaurate (catalyst, DBTDL), 3-(trimethylsilyl)propionic-2,2,3,3-d 4 acid sodium salt (TSP), trifluoroacetic acid (TFA), amphotericin B and curcumin (from *Curcuma Longa,* 368.4 Da) were purchased from Merck/Sigma Aldrich (Milan, Italy). All solvents were purchased from Carlo Erba Reagents (Milan, Italy). P407 and F68 were dehydrated at 100 °C for 8 hours at low pressure (i.e., 150-200 mbar) and then maintained at 40 °C under vacuum until use. CDM and NBoc chain extenders were dried into a desiccator (1-5 mbar) at room temperature (i.e., *ca.* 25 °C), while HDI was distilled under vacuum. 1,2-dichloroethane (DCE) was used as solvent for PEU synthesis after drying over activated molecular sieves (Merck/Sigma Aldrich, Milan, Italy, activation at 120 °C, atmospheric pressure) under N_2 atmosphere for at least 8 hours. α-CDs (hereafter simply coded as "CDs") were obtained from TCI Chemical Europe (Zwijndrecht, Belgium) and used as supplied.

2.2 Synthesis of PEUs

PEUs were synthesized as reported in previous works.[63,64,66–68] Briefly, the process was carried out in two steps. The first one consisted in the pre-polymerization of the macrodiol (P407 or F68, 20% w/v in anhydrous DCE) with HDI (2:1 molar ratio with respect to the macrodiol) for 2.5 hours at 80 °C in the presence of DBTDL catalyst (0.1% wt with respect to the macrodiol). Subsequently, the second step was conducted at 60 °C for 1.5 hours through the addition of the chain extender (CDM or NBoc, 1:1 molar ratio with respect to the macrodiol) after dissolution in anhydrous DCE (3% w/v). At the end of these two steps, the polymer solution was cooled down to room temperature and methanol was added to passivate any unreacted isocyanate group. Then, PEU solution was precipitated in petroleum ether (4:1 volume ratio with respect to total DCE volume) under stirring and dried overnight under a fume hood at room temperature. Subsequently, the PEU was again solubilized in DCE at 20% w/v and purified in a diethyl ether-methanol mixture (98:2 v/v, 5:1 volume ratio with respect to DCE) to remove any unreacted reagent, low molar mass by-products and residual catalyst. Finally, the polymer was collected through centrifugation at 0 °C and 6000 rpm for 20 minutes (Hettich, Mikro 220R) and kept under a fume hood overnight to ensure complete drying. The synthesized PEUs were then stored under vacuum at 3 °C. Depending on the reagents, three PEUs were synthesized and coded with the

acronyms CHP407, NHP407 and NHF68, where “C”, “N” and “H” identify CDM, NBoc and HDI, respectively, meanwhile P407 and F68 refer to PEU constituent macrodiol.

2.3 De-protection of NBoc-containing PEUs

Boc-group cleavage was carried out through acid treatment of NHP407 and NHF68 PEUs, as recently reported by Boffito *et al.*.[65] In detail, NBoc-based PEU was solubilized (10g) in chloroform (CF) at room temperature and 250 rpm for 2.5 hours. Then, trifluoroacetic acid (TFA) was added to the polymer solution to reach the operative concentration of 4% w/v in a CF-TFA (90:10 v/v) mixture. The reaction was conducted for 1 hour and then the solution was concentrated using a rotary evaporator (RII Rotavapor, Buchi). Subsequently, the concentrated polymeric solution was washed twice with 100 ml of CF; then, 200 ml of distilled water were added and the resulting suspension was maintained under vigorous stirring overnight at 3 °C. Finally, dialysis was performed (cellulose membrane, cut-off 10-12 kDa, Sigma Aldrich, Milan, Italy) against distilled water at 3 °C for 2 days in order to remove any TFA traces. The dialyzed solution was then freeze dried (Martin Christ ALPHA 2-4 LSC, Germany) for 2 days and the collected polymer was stored under vacuum at 3 °C until use. Hereafter, Boc-deprotected PEUs resulting from the acid treatment of NHP407 and NHF68 will be referred to with the acronyms SHP407 and SHF68, respectively.

2.4 Chemical characterization of PEUs

2.4.1 Attenuated Total Reflectance – Fourier Transformed Infra-Red (ATR-FTIR) spectroscopy

ATR-FTIR spectroscopy characterization was performed to prove the correct formation of urethane domains. Analyses were conducted on PEU powder at room temperature using a spectrometer (Perkin Elmer Spectrum 100) equipped with an ATR accessory with diamond crystal (UATR KRSS). Spectra were obtained as average of 16 scans at a resolution of 4 cm^{-1} in the wavenumber range from 4000 to 600 cm^{-1}. Recorded spectra were then analyzed through the Spectrum software (Perkin Elmer). Macrodiols used for PEU synthesis were also analyzed for comparison.

2.4.2 Size Exclusion Chromatography (SEC)

PEUs were characterized in terms of their molar mass distribution to assess the successful polymerization of the involved reagents. Tests were performed through an Agilent Technologies 1200 Series (California, USA) SEC integrated with a Refractive Index detector and two

chromatographic columns (Waters Styragel HR1 and HR4). N,N-dimethylformammide (DMF, HPLC grade, Carlo Erba Reagents, Milan, Italy) added with lithium bromide (0.1% w/v, ReagentPlus, >99%, Merck/Sigma Aldrich, Milan, Italy) was used as mobile phase at 0.5 ml min^{-1} flow rate. Number average molar mass ($\overline{M}_n$), weight average molar mass ($\overline{M}_w$) and dispersity index (D = $\overline{M}_w/\overline{M}_n$) of PEUs were obtained through the Aligent ChemStation software utilizing a calibration curve based on PEO standards with peak molecular weight ($\overline{M}_p$) in the range 982-205500 Da. Analyzed samples were prepared by solubilizing 2 mg of PEUs in 1 ml of mobile phase followed by filtration through 0.45 µm poly(tetrafluoroethylene) (PTFE) syringe filters (LLG International, Meckenheim, Germany).

2.4.3 Proton Nuclear Magnetic Resonance (^{1}H-NMR) spectroscopy

^{1}H-NMR characterization was performed on native PEUs (CHP407, NHP407 and NHF68) and de-protected derivatives (SHP407 and SHF68) to prove the successful synthesis of both P407- and F68-based polymers, as well as to assess whether any degradative phenomena occurred during Boc-group cleavage reaction. The spectra were obtained in deuterium oxide (D_2O, 99.8%, Sigma Aldrich, Milan, Italy) through an Avance III Bruker spectrometer equipped with a 11.74 T superconductor magnet (500 MHz 1H Larmor frequency), a Bruker BBFO direct probe and a Bruker BVT 3000 unit for temperature control. 1 mM TSP in D_2O in a sealed capillary was inserted in the NMR tube and used as reference for the zero of the chemical shift scale. All tests were performed at 25 °C and the spectra resulting from the average of 12 scans (10 seconds relaxation time) were referred to D_2O peak at 4.675 ppm. The registered spectra were further elaborated using MNova software (Mestrelab Research, S.L, Spain, www.mestrelab.com).

2.4.4 Exposed primary amine quantification through Orange II Sodium Salt colorimetric assay

Primary amino groups in Boc-deprotected PEUs (i.e., SHP407 and SHF68) were quantified according to the protocol developed by Laurano and colleagues.[64] In detail, PEUs were solubilized (0.04% w/v) in double distilled water (ddH_2O) containing Orange II Sodium Salt (Sigma Aldrich, Milan, Italy) at 0.175 mg ml^{-1} concentration previously adjusted at pH 3 and then incubated at room temperature (i.e., 25 °C) for 18 hours protected from any source of light. Unreacted reagents were then removed through dialysis (cellulose membrane cut-off 10-12 kDa, three complete dialysis medium refreshes per day) for 3 days in the dark utilizing ddH_2O as dialysis medium and then the samples were freeze dried (Martin Christ ALPHA 2-4 LSC). The quantification was performed after dye detachment from amino groups through freeze-dried

polymer solubilization in ddH_2O at pH 12 for 2 hours at room temperature, followed by centrifugation at 15 °C and 6000 rpm for 10 minutes. The supernatants of the samples were then analyzed with a UV-Vis spectrophotometer (Perkin Elmer Lambda 25 UV/VIS spectrometer, Waltham, MA, USA) in the wavelength range between 700 and 400 nm and by measuring the absorbance of dye characteristic peak at 485 nm. A calibration curve for the quantification of free amino groups was obtained through Orange-based standard samples prepared in ddH_2O (pH 12) at concentrations ranging from 1.75 to 29.2 μg ml^{-1}. In order to subtract potential absorbance contribution due to dye adsorption to polymer chains, NHP407 and NHF68 control samples were also analyzed according to the same protocol.

2.4.5 Critical Micellar Temperature (CMT) evaluation

CMT was evaluated with the aim to thoroughly understand PEU thermo-responsiveness in aqueous solution at low concentration. Briefly, 1,6-diphenyl-1,3,5-hexatriene (DPH, Sigma Aldrich, Milan, Italy) fluorescent dye (4×10^{-4} mol L^{-1} in methanol) was added to PEU aqueous solutions (1% w/v in PBS or ddH_2O) in order to detect the temperature-driven micelle formation by quantifying the incremental absorbance (Perkin Elmer Lambda 25 UV/VIS spectrometer, Waltham, MA, USA) in the wavelength range of 350-360 nm resulting from the progressive solubilization of DPH into micelle cores. The tests were conducted in the range of temperatures from 5 to 40 °C at a rate of 1 °C per step with 5 minutes equilibration time. The peak absorbance at 356 nm was then graphed as a function of temperature and CMT values were estimated as the intercept between the data trend lines defined before and after the inflection point.[69,70]

2.5 Preparation and characterization of PEU- and CD-based supramolecular (SM) complexes

2.5.1 Preparation of SM crystalline complexes

PEU- and CD-based inclusion complexes (IC) were prepared in ddH_2O by mixing the two components in solution. In detail, PEUs were weighted at specific amounts and solubilized overnight in ddH_2O at 3 °C. Simultaneously, a solution containing CDs at 14% w/v was prepared in ddH_2O and added to PEU samples and the obtained mixtures were then homogenized using a vortex stirrer (40 Hz for 20-30 seconds). Subsequently, in order to allow SM complexation, the samples were incubated at room temperature (i.e., 25 °C) for 72 hours obtaining crystalline suspensions. To separate PPR-based crystals, the samples were centrifuged at 4500 rpm and 10 °C for 15 minutes, the resulting supernatants were thrown away meanwhile the pellets were quenched with liquid nitrogen. A wide range of compositions based on various contents of PEUs

(1 and 2% w/v) and CDs (ranging between 7 and 12% w/v) was investigated aiming at selecting those able to yield a mass of SM crystals greater than 30%. Powders composed of ICs were then obtained through freeze drying (Martin Christ ALPHA 2-4 LSC, Germany) for 24 hours. SM samples have been coded as follows: PEU X%-SM Y%, where X is the PEU concentration and Y is the content of CDs with respect to the total amount of EO domains (assuming a molar ratio of 2 EO groups every 1 CD molecule).

2.5.2 X-Ray powder Diffraction (XRD) analysis

The collected crystalline matter was characterized by XRD analysis to assess the successful formation of SM crystals based on PEUs and CDs. Analyses were performed through an X-Ray diffractometer Siemens D5005 with Bragg-Brentano geometry and vertical theta-theta goniometer (the anode and detector rotate while specimen holder is fixed). The setup parameters were Cu Kα (1.542 Å) anode at 40 kV, 40 mA, Ni-filter, 2θ range from 5° to 30°, scanning rate 0.1 deg $step^{-1}$, acquisition time 10 s $step^{-1}$. The same protocol was applied also to PEU control samples for comparison.

2.5.3 Attenuated Total Reflectance – Fourier Transformed Infra-red (ATR-FTIR) Spectroscopy

ATR-FTIR analysis was performed on SM samples to assess the presence of any shift in specific chemical domains of the involved components. Spectra were obtained from the average of 32 scans in the spectral range from 4000 to 600 cm^{-1} at a resolution of 1 cm^{-1}. All the analyses were performed at ambient temperature on three replicates that were averaged, and control samples were also tested as references.

2.5.4 Proton Nuclear Magnetic Resonance (^{1}H-NMR) Spectroscopy

^{1}H-NMR characterizations of crystalline SM complexes were performed as reported before for pure PEUs to assess the presence of both PEUs and CDs in the collected crystallin matter. Samples were prepared through solubilization of SM crystalline powders in D_2O (Sigma Aldrich, Milan, Italy) at a concentration of 5 mg ml^{-1} and the obtained spectra were elaborated using MNova software (Mestrelab Research, S.L, Spain, www.mestrelab.com).

2.6 Preparation and characterization of PEU- and CD-based SM hydrogels

2.6.1 Preparation of SM hydrogels

SM hydrogels (1 ml) were formulated in PBS (pH 7.4, Merck/Sigma Aldrich, Milan, Italy) by mixing PEU and CD solutions. PEUs were dissolved at specific concentrations in Bijou sample containers (17 mm diameter, 7 ml, Carlo Erba Reagents, Milan, Italy) at 3 °C overnight. A CD solution at 14% w/v in PBS was prepared and added to the previously prepared PEU solutions. Immediately after mixing, the samples were stirred using a vortex (40 Hz for 20-30 seconds) and then incubated at room temperature (i.e., 25 °C) to allow the development of SM networks. New formulations based on blends of CHP407 and SHF68 solutions containing CD at 10% w/v were also designed. The weight ratio between CHP407 and SHF68 was maintained at 80/20 w/w, while the overall PEU concentration was the same as that of samples based on a single PEU (i.e., ranging from 1% to 5% w/v). The samples were coded as PEU X% - CD Y%, where X and Y are the concentrations (% w/v) of PEU and CDs, respectively. For the blends composed of CHP407 and SHF68, the utilized codes were BLEND X% - CD Y%, where X and Y are defined similarly to single PEU-based samples.

2.6.2 Qualitative evaluation of gelation time and phase-separation in isothermal conditions

The required time for complete gelation of SM hydrogels was estimated at room temperature (25 °C) through visual inspection as a qualitative evaluation of their ability to form solid networks. In detail, samples were visually analyzed at defined time frames (every 1 and 5 minutes up to 1 hour and then every 10 minutes), through vial inversion and analysis of the status of the gelling solutions, i.e., possible presence of hydrogel flow along vial walls. “Gel” condition was determined by the absence of viscous flowing within 30 seconds of observation.

2.6.3 Rheological characterization

Mechanical properties of PEU-based SM hydrogels were investigated through rheological characterization utilizing a stress-controlled rheometer (MCR302, Anton Paar GmbH, Graz, Austria) equipped with a Peltier temperature control unit and a 25 mm parallel plate configuration. The hydrogels (PEU concentration ranging between 1 and 5% w/v and CDs at 10% w/v) were loaded through injection (5 ml syringe, 2 mm needle, approx. 0.4 ml) onto the rheometer lower plate previously set at 25 °C. Sample thickness was set at 0.6 mm and the temperature was equilibrated for 10 minutes before any test. During the tests, the value of normal force was set at 0 N. Strain sweep tests were carried out at 37 °C and at an angular frequency of 1 rad s^{-1} within the strain range from 0.01 to 500%. For each analyzed sample, the same strain sweep test was performed again after 15 minutes re-equilibration at 37 °C, to assess the ability of the studied hydrogels to recover their mechanical properties after relevant strain (500%) application.

Frequency sweep tests were performed in the range of the linear viscoelastic region (i.e., 0.1% strain) at three different temperatures (25, 30 and 37 °C) in the domain of angular frequencies between 100 and 0.1 rad s^{-1}. Self-healing strain test were performed a 1 Hz frequency to observe the dynamic self-healing ability of hydrogels when a variable strain was applied cyclically by alternating for three times low (0.1%, recovery phase, 120 seconds) and high (100%, rupture phase, 60 seconds) deformations. Finally, the initial recovery phase was applied again to evaluate sample residual mechanical properties.

2.6.4 Swelling and stability of hydrogel networks

Hydrogel behavior and responsiveness in contact with an aqueous environment was evaluated through swelling and dissolution tests. In detail, 1 ml samples were prepared in Bijou sample containers (7 ml capacity with an inner diameter of 17 mm) as previously described. In order to ensure complete gelation, samples were incubated overnight at room temperature before test beginning. Samples were weighted (W_{gel_i}) and acclimatized at 37 °C for 15 minutes. Then, 1 ml of PBS (37 °C) containing amphotericin B (1.25 µg ml^{-1}, Merck/Sigma Aldrich, Italy) was gently added to each sample. At defined time points (6 h, 24 h, 3 days and 5 days), samples were collected, weighted after removal of the residual PBS (W_{gel_f}), freeze dried and weighted again ($W_{dried_gel_f}$). To simulate fluid renewal, refreshes of eluates were performed trice a week. PBS absorption (PBS Absorption %) was calculated as reported in equation 1, while hydrogel dissolution (Weight Loss %) was obtained from equation 2 using control samples that were freeze dried (Martin Christ ALPHA 2-4 LSC, Germany) immediately after preparation ($W_{dried\ gel_i}$) as reference.

$$PBS\ Absorption\ \% = \frac{W_{gel_f} - W_{gel_i}}{W_{gel_f}} \times 100 \qquad \text{Eq.1}$$

$$Weight\ Loss\ \% = \frac{W_{dried\ gel_i} - W_{dried\ gel_f}}{W_{dried\ gel_i}} \times 100 \qquad \text{Eq.2}$$

In addition, hydrogel behavior was further investigated by calculating the swelling ratio at each time point. This represents a powerful instrument to determine the ratio between the water and the polymer fractions constituting the hydrogels over time. Equation 3 was implemented to calculate swelling ratio and control samples were prepared and utilized as reference (swelling ratio equal to 1).

$$Swelling\ ratio = \frac{W_{gel_f} - W_{dried\ gel_f}}{W_{dried\ gel_f}} \qquad \text{Eq. 3}$$

Analyses were conducted in quintuplicate and results are reported as mean ± standard deviation.

2.6.5 Cytotoxicity evaluation

Cytotoxicity tests were performed according to ISO10993 on hydrogels composed of PEU at 1 and 5% w/v concentration and CDs at 10% w/v concentration. In detail, samples containing 250 mg of SM hydrogels were prepared in Bijou sample containers (7 ml, 17 mm inner diameter), sterilized through UV irradiation (290 nm) for 30 minutes and acclimatized at 37 °C for 15 minutes. Subsequently, 1 ml of Dulbecco's Modified Eagle Medium (37 °C, high glucose, Carlo Erba Reagents, Milan, Italy) with foetal bovine serum (10% v/v, Carlo Erba Reagents, Milan, Italy) was added every 100 mg of weighted SM hydrogel. Samples were incubated at 37 °C for 24 hours and then the elutes were collected. In parallel, NIH 3T3 cell line (Atcc, USA) was seeded and cultured on a 96 well plate (20'000 cell $well^{-1}$, 100 µl cell culture medium), for 24 hours at 37 °C (5% CO_2) using the same medium as for the eluates. Then, the culture medium was withdrawn, and the obtained hydrogel eluates (100 µl) were added and incubated in contact with cells for 24 hours. Finally, the medium was completely refreshed with a new one (100 µl) containing resazurine (0.1 mg ml^{-1}, Sigma Aldrich, Milan, Italy) and the plate was incubated for 1 hour at 37 °C. Cell viability was evaluated through a multimode plate reader (Perkin Elmer Victor X3) by measuring the reduced form of resazurine at 595 nm after excitation at 530 nm. All the experiments were referred to control samples (100 % viability).

2.6.6 Encapsulation of curcumin and characterization of drug-loaded samples

In order to encapsulate curcumin (Cur) into SM hydrogels (1 ml) preventing any potential drug degradation phenomena,[71,72] the required amount of CDs to form hydrogels was divided in two fractions. The first 50% (%v) of CDs was solubilized in PBS (14% w/v) as described above and firstly added and mixed to PEU solutions, while the remaining 50% was dissolved in ddH_2O (pH 5.5 – 6, 14% w/v) and added with Cur at 225 µg ml^{-1} concentration. In order to achieve a complete solubilization, ultrasound sonication (52 W, 20 kHz, Vibracell VCX130, Sonics, USA) was applied for 3 minutes using a probe while stirring to properly dissolve any powder aggregate of curcumin in the CD solution. Then, CD solution containing Cur was added to the hydrogel samples reaching the selected CD (10% w/v) and PEU (1 and 3% w/v) concentrations and a Cur content of 80 µg ml^{-1}. Finally, samples were maintained at room temperature (25 °C) for 48 hours to ensure gelation.

A complete rheological characterization was performed as described above in paragraph 2.6.3 in order to evaluate potential effects of solvent composition (pure PBS *vs*. a mixture of PBS and

ddH$_2$O) and Cur encapsulation on SM hydrogel properties. The acronyms PEU X%-CD Y%-PBS/H$_2$O and PEU X%-CD Y%-Cur 80 mg/ml were utilized to indicate the samples characterized by the single contribution of solvent composition and the additional presence of curcumin, respectively.

Release studies were performed after equilibration of hydrogel samples (1 ml in Bijou containers with a 17 mm diameter) at 37 °C for 15 minutes. Then, 1 ml of PBS (37 °C) was gently added to each sample. Elutes were collected at specific time points (2, 4, 6, 24, 48, 72 and 96 hours) and completely refreshed with fresh PBS. Immediately after collection, 200 µl of the obtained release media were transferred into a 96 well plate and quantified through a multimode plate reader (Perkin Elmer Victor X3) by measuring the absorbance at 450 nm. Cur quantification was performed by referring to a calibration curve based on standards with Cur concentration in the range 1-10 µg ml^{-1}. The Korsmeyer–Peppas model (Power law) was then applied to release data collected within the first 6 hours of observation with the aim to better describe the occurring release mechanism.[73] In detail, equation 4 was implemented to calculate the release exponent *n:*

$$\frac{M_t}{M_\infty} = Kt^n \quad ; \quad Log\left(\frac{M_t}{M_\infty}\right) = nLog(t) + Log(K) \qquad \text{Eq. 4}$$

where M_t is the mass of released drug at a defined time step *t*, M_∞ is the total encapsulated curcumin payload and K is a constant of incorporation of structural modification (also considered as the release velocity constant). For cylindrical samples, *n* values of 0.45 and 0.89 indicate a release mechanism based on diffusion or swelling, respectively. Values ranging between 0.45 and 0.89 represent a combination of the above-mentioned release phenomena, resulting in an anomalous transport. *n* values greater than 0.89 describe an extreme way of transport, where inner tensions of hydrogel network are generated by a relevant mass exchange with the external environment and solvent absorption.

2.7 Statistical Analysis

Statistical analysis was conducted through GraphPad Prism 8 for Windows 10 (GraphPad Software, La Jolla, CA, USA; www.graphpad.com). Two-way ANOVA analysis coupled with Bonferroni multiple comparison test was utilized to compare results, and statistical significance was defined according to Boffito *et al.*.[66]

Significance level were assigned depending on p-values: $p<0.0001$ Extremely significant (****), $0.0001<p<0.001$ Extremely significant (***), $0.001<p<0.01$ Very significant (**), $0.01<p<0.05$ Significant (*), $p\geq0.05$ Not significant (ns).

3. Results

3.1 Physico-chemical characterization of PEUs

3.1.2 ATR-FTIR spectroscopy and SEC

Infra-red spectroscopic analyses were performed to assess the successful formation of urethane domains. Figure S1 of supplementary material reports the spectra of PEUs and the native Poloxamers (P407 and F68) used for their synthesis. The effective urethane bond formation was proved by the presence of new vibration bands at 1720 cm^{-1}, indicating the stretching of free carbonyl (C=O) groups, and at 1530 cm^{-1} due to the simultaneous excitation of N-H (bending) and C-N (stretching) bonds. In addition, a wide peak related to N-H stretching was detected at 3350 cm^{-1}. The absence of any peak around 2200 cm^{-1} confirmed the complete conversion of isocyanate groups into urethane bonds. Moreover, the typical Poloxamer/Pluronic absorption peaks were detected proving the successful synthesis of Poloxamer/Pluronic-based PEUs: CH_2 bands at 1250 cm^{-1} (stretching) and 2880 cm^{-1} (rocking), while the peak at 1100 cm^{-1} was due to the stretching of C-O-C domains. SEC results are summarized in Table 1. Relying on the assumption that the characteristic error of SEC results is around 10%,[74] PEU molar masses were measured to be significantly greater with respect to their native Poloxamers. Moreover, molar masses of all P407-based PEUs did not show significant differences between each other, as well as for F68-based ones. These results proved the consistency of the performed synthesis method and the absence of any degradation phenomena after Boc-cleavage treatments, according with previous works.[64,65] Slightly higher molar masses were detected for P407-based PEUs with respect to F68-based ones, in agreement with the higher molar mass of the Poloxamer used for their synthesis. Finally, a good consistency was also obtained in terms of dispersity indexes, which turned out to be 1.8 for all PEUs.

	Number average Molar mass ($\times10^4$ Da)	***Weight average Molar mass ($\times10^4$ Da)***	***Dispersity index (D)***
P407	0.80	0.95	1.2
CHP407	3.10	5.40	1.8
NHP407	2.70	4.70	1.8
SHP407	2.90	5.30	1.8

F68	0.63	0.68	1.1
NHF68	2.20	3.80	1.8
SHF68	2.40	4.00	1.8

Table 1: *Number and weight average molar mass (M_n and M_w) and dispersity index (D) values as estimated by SEC for the synthesized PEUs and the native Poloxamers used for their synthesis.*

3.1.2 Proton nuclear magnetic resonance (^{1}H-NMR) spectroscopy and free primary amine quantification

^{1}H-NMR characterization represents a valuable tool to assess PEU synthesis success and to establish whether the procedure of Boc-cleavage has induced any chemical degradation of PEU backbone and has been successfully performed. As reported in figure 1, no differences were detected in the spectra of PEUs based on the same macrodiol, thus suggesting a consistent synthesis procedure and even no variations in their molecular structures, in agreement with SEC and ATR-FTIR results. However, PEUs treated to expose primary amines (i.e., SHP407 and SHF68) showed an evident intensity decrease of the peak related to Boc groups at about 1.36 ppm with respect to their native counterparts (i.e., NHP407 and NHF68, respectively), thus highlighting the effectiveness of the deprotection procedure. On the other hand, some differences can be observed between the ^{1}H-NMR spectra of P407- and F68-based PEUs. In detail, the peak arising from Boc groups in NHF68 spectrum showed a higher intensity if compared to the one in NHP407 (approx. 50% greater) considering the bands related to HDI domains (i.e., between 1.46 and 1.37 ppm) as a reference. This result suggested an improved chain extension process in the synthesis of NHF68 compared to NHP407, probably due to a higher reactivity of smaller F68-based pre-polymers that resulted from the first step of polymerization. This hypothesis was further corroborated by the correlation existing between the deprotection yields, evaluated by ^{1}H-NMR spectroscopy, and the primary amine quantification by Orange II sodium salt colorimetric assay. Indeed, Boc cleavage procedure applied to NHP407 resulted in an almost completed deprotection of available primary amines (deprotection yield > 90%) along PEU backbone, while a yield of 83% was obtained from NHF68. It is likely that this difference could be ascribed to the higher number of NBoc chain extenders present in NHF68 with respect to NHP407. As a matter of fact, the exposed primary amines in SHP407 and SHF68 resulted to be 3.5E18 ± 5.4E17 NH_2/g_{SHP407} and 1.7E19 ± 3.9E18 NH_2/g_{SHF68}, respectively. The exposure of a relevant number of free amino groups along polymer chains makes such PEUs promising functional macromolecules for drug delivery applications. Indeed, it is well-known that -NH_2 groups can be exploited to perform bulk functionalization procedures through carbodiimide chemistry or using specific coupling molecules such as genipin[64,75] or to confer pH responsiveness to acid environments,[65] such as tumor

or acute inflammation milieus.[76,77] Indeed, amino-functionalized amphiphilic polymers represent highly interesting systems for the encapsulation and delivery of therapeutic agents into tumor environments with improved bioavailability and efficacy.[78] In this regard, SHP407 has already been applied to successfully design thermo-sensitive and pH-responsive hydrogels for the encapsulation of smart carriers (i.e., mesoporous silica nanoparticles) surface functionalized through a self-immolative polymeric coating, which was engineered to degrade under acid conditions to trigger the release of loaded therapeutic agents.[65]

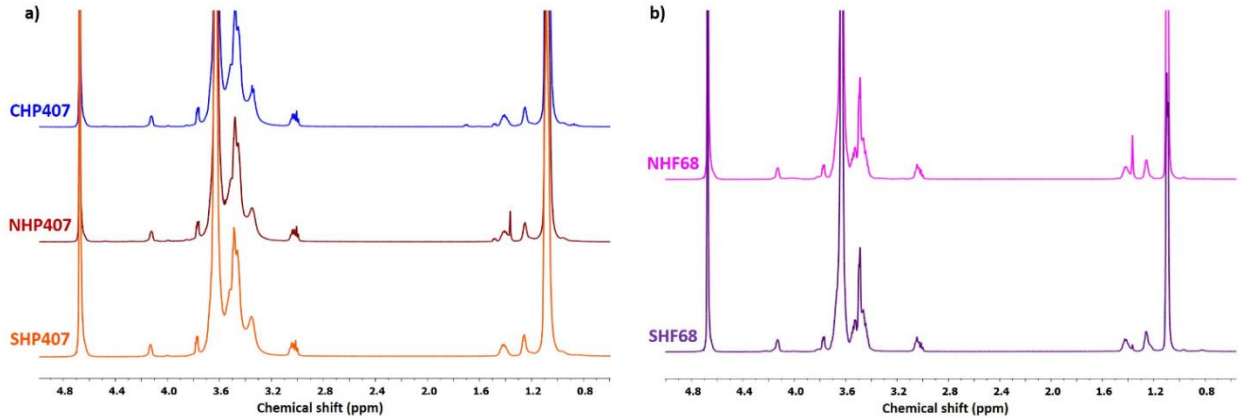


Figure 1: *^{1}H-NMR spectra of a) P407-based (CHP407 (blue), NHP407 (brown) and SHP407 (orange)), and b) F68-based (NHF68 (pink), SHF68 (purple)) PEUs.*

3.1.3 Critical Micellar Temperature (CMT) evaluation

In a watery environment, amphiphilic PEUs are expected to form polymeric micelles showing a hydrophobic core and a hydrophilic external layer upon thermal stimulus. In this regard, CMT evaluation allows to better understand the extent of PEU thermo-responsiveness, which is an important factor even for the formation PPR-based crystals. In fact, previous works hypothesized that the hydrophobic interactions leading to micelle formation exert a stabilizing function on SM hydrogel formation.[58,59,79] Additionally, also other solutes (i.e., salts) can play a fundamental role in micelle assembly and formation kinetics. Indeed, it has been demonstrated that the presence of ionic species can affect the micelle formation process by decreasing the CMT value, acting as a further stabilizing element.[80,81] Hence, in order to get further insight on the self-assembly process of the here-developed PEUs, CMT evaluation was conducted by solubilizing the synthesized materials in PBS or ddH_2O at 1% w/v concentration. Figure 2 reports absorbance values measured at 356 nm as a function of temperature and the two trend lines used for CMT

definition for all PEUs solubilized in PBS. It is evident that the two constituting macrodiols (i.e., P407 and F68) resulted in totally different PEU behaviors. Indeed, P407-based PEUs showed a sharp increase of the signal due to DPH solubilization into micelle cores. This behavior can be correlated with the marked hydrophobic nature of P407. The obtained CMT values for CHP407, NHP407 and SHP407 samples are reported in table 2 and resulted to be in a restricted temperature range between 19.5 and 20.1 °C, thus indicating a similar thermo-responsiveness for these PEUs mainly due to the overall properties resulting from the chain-extension of P407 domains. Differently, F68-based PEUs did not show any micellization phenomena: no signal variations were detected in NHF68 sample, while a slight increase of absorbance was observed in SHF68-based solution. It is likely that the dimension and the relative amount of PPO domains (i.e., c.a. 20% wt.) were not suitable for micelle formation below the physiological temperature (i.e., 37 °C), although the synthesis process resulted in highly chain extended molecules, as discussed before.

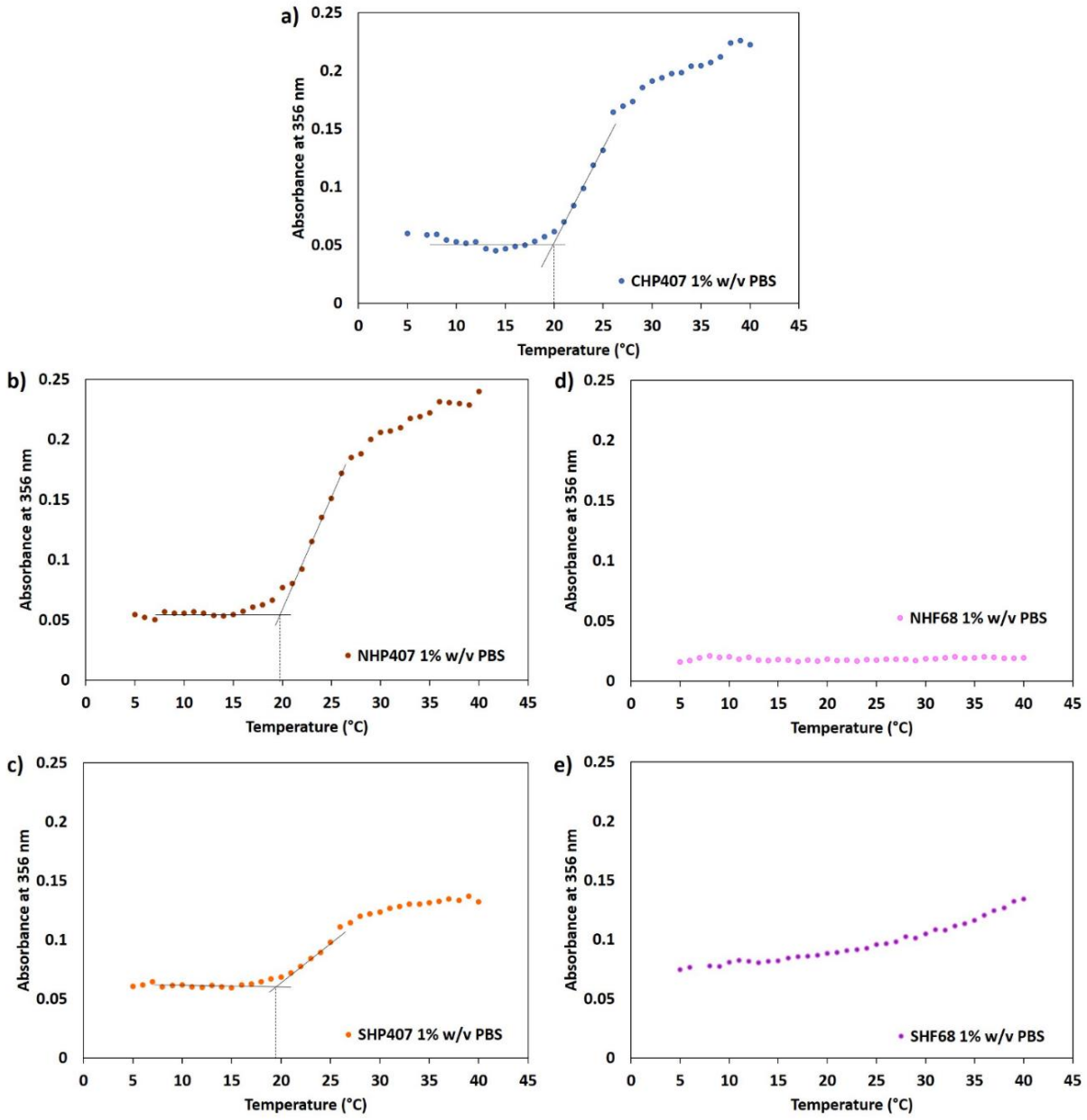


Figure 2: *Absorbance measured at 356 nm as a function of temperature for a) CHP407 (blue), b) NHP407 (brown), c) SHP407 (orange), d) NHF68 (pink), and e) SHF68 (purple) solutions (1% w/v) in PBS. Trend lines used for CMT evaluation are reported in black.*

PEU	CMT in PBS (°C)	CMT in ddH_2O (°C)
CHP407	20.1	21.5
NHP407	19.8	22.0
SHP407	19.5	22.3
NHF68	-	-
SHF68	-	-

Table 2: *CMT values of PEU-based solutions (1% w/v) in PBS and ddH_2O.*

PEU solutions in ddH_2O showed similar trends (Figure S2 of supplementary material). However, their CMT values were slightly higher compared to those evaluated for samples prepared in PBS due to the absence of salting out effect, as reported in table 2.

3.2 Physico-chemical characterization of SM complexes

3.3.1 X-ray powder diffraction (XRD) analysis

XRD tests were performed with the aim to demonstrate PEU ability to form a specific supramolecular network based on packed PPRs into channel-like crystals. PEUs were able to form turbid suspensions upon mixing with CDs in water. The white crystalline matters were separated through centrifugation and their diffractograms were recorded and reported in figure 3.

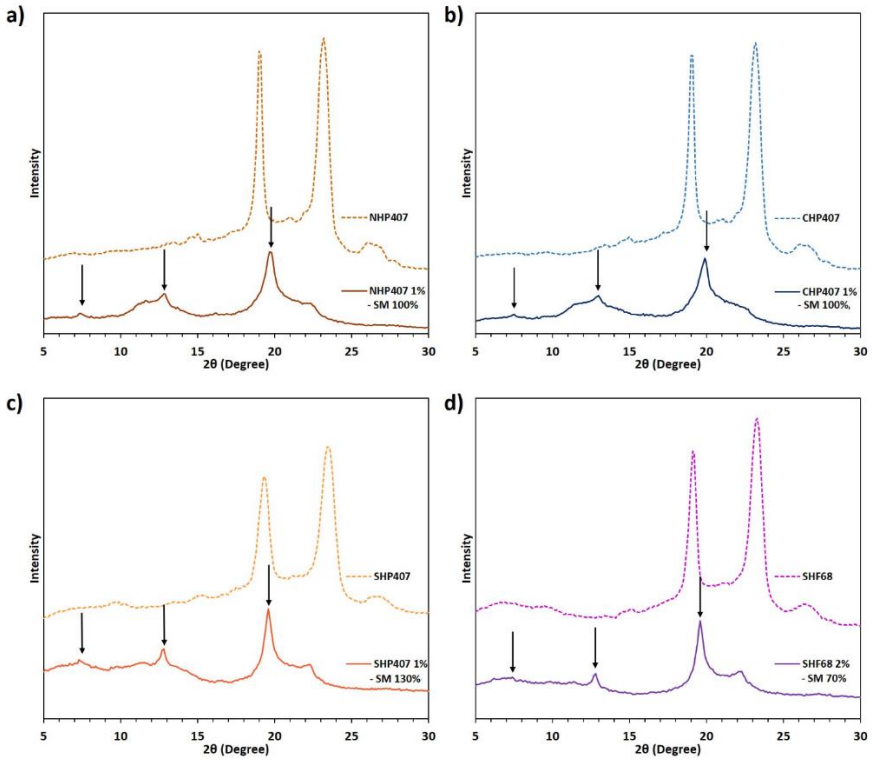


Figure 3: *XRD spectra of pure PEU powders (dashed lines, light color) and the corresponding SM crystalline powders (continuous lines, dark color); a) NHP407 (brown), b) CHP407 (blue), c) SHP407 (orange), and d) SHF68 (purple). The typical peaks (approx. 2θ equal to 7.2°, 12.8° and 19.8°) of SM crystals composed of packed PPRs are highlighted by vertical black arrows.*

The resulting crystalline powders were characterized by diffractograms having specific peaks around 2θ equal to 19.8°, 13° and 7.6°, which indicate an evident formation of hexagonal channel-like supramolecular crystals.[63,82] The absence of multiple reflections confirmed that all involved

CDs were employed in the formation of PPR-based SM crystals. Pure PEU patterns were also registered as control and exhibited two peaks around 19.1° and 23.2°, as typical of most PEO-based polymers[82] (Figure 3). These data demonstrated the possibility to successfully employ PEUs with different chemical structures as building blocks for SM systems, in agreement with our previous findings.[63] Interestingly, the here-investigated plethora of PEUs exhibited significantly different behaviors in terms of supramolecular crystallization. In fact, CHP407 and NHP407 SM systems for XRD analysis were formulated at a PEU concentration of 1% w/v and a CD content to theoretically cover 100% of available domains of EO (i.e., 7.6% w/v), producing yields of crystallization around 58 ± 0.5% and 30 ± 0.5%, respectively.[63] Differently, SHP407, NHF68 and SHF68 required higher polymer and/or CD concentrations to achieve a comparable yield of crystallization (i.e., crystalline powder yield > 30%). In detail, the obtained compositions were the following: SHP407 1% - SM 130% (i.e., 10% w/v CD concentration, 74.4 ± 1.5 % yield) and SHF68 2% - SM 70% (i.e., 12% w/v CD concentration, 84.8 ± 0.4 % yield). NHF68-based solutions did not form a sufficient amount of crystalline powder (yield < 10%) in none of the tested conditions (i.e., PEU concentration at 1 or 2% w/v and CD content ranging between 7 and 12% w/v). From a general point of view, these results can be correlated with the different PEU thermo-responsiveness, as previously shown through CMT results. In fact, it is most likely that the samples based on P407 showed a relevant formation of crystalline matter at lower polymer and CD contents due to their higher ability to form hydrophobic interactions that acted as stabilizing elements for PPR formation and crystallization. On the other hand, although F68-based PEUs exhibited slightly lower molar masses compared to P407-based ones (i.e., $\overline{M}_n$ approx. 20% lower with respect to P407-based ones) which in principle would favor the assembly process, they were also composed of smaller hydrophobic domains which probably represented an important hindering element to SM crystal formation. Nonetheless, SHF68-based solutions resulted in a significantly higher crystallization yield with respect to NHF68-based ones. In addition to the above-mentioned common factors, this different behavior may be correlated to the intrinsic hindrance resulting from the presence of a great number of pendant Boc groups along NHF68 polymer chains. Interestingly, an opposite tendency was observed for NHP407 and SHP407. Indeed, the former produced a relatively higher amount of SM crystalline powder (i.e., around 30% ± 0.5%) at lower PEU and CD concentrations (i.e., 1% w/v and 7.6% w/v, respectively) when compared to the latter, which did not produce a sufficient yield (i.e., < 10%) in the same conditions. Hence, the system based on SHP407 at 1% w/v concentration required higher CD content (i.e., 10% w/v) to yield a sufficient mass (i.e., > 30%) of SM crystal, as previously discussed. The presence of a lower number of pendant Boc groups along NHP407 chains probably favored the

formation of additional hydrophobic interactions with PPO domains as stabilizing physical crosslinks for SM crystallization, without significantly impeding CD threading along polymer chains.

3.2.2 ATR-FTIR characterization

In order to further prove the co-presence of PEUs and CDs in the crystalline matter obtained from SM suspensions in ddH_2O, ATR-FTIR characterizations were conducted on the same samples used for XRD crystallography. Figure 4 reports the ATR-FTIR spectra of PEUs and CDs at their native state compared with SM samples. The co-presence of typical vibration bands of both PEU and CDs were detected in all the analyzed samples. For instance, CD characteristic peaks at 1075, 1155 and 2954 cm^{-1} (C-O, C-O-C and CH stretching vibration, respectively) were identified in all SM sample spectra. Moreover, even the peak related to the symmetric and asymmetric vibration of -OH groups of CDs around 3308 cm^{-1} was detected in SM samples, but it was characterized by a general upshift towards higher wavenumbers (up to 3340 cm^{-1}). This peculiarity is correlated to the channel-like conformation of CDs involved in the formation of PPR-based crystals, as reported in previous works.[83] More in detail, CD arrangement into crystallized PPRs consisted in a linear head-tail molecular disposition rather than in cage-like crystals. To what concerns typical PEU vibration bands, the peak related to the stretching of carbonyl groups (C=O) at 1720 cm^{-1} resulted to be upshifted in SM sample spectra (up to 1740 cm^{-1}), indicating inhibited packing and crystallization of PEU chains. Interestingly, the entity of these shifts was remarkably lower for SHF68 PEU sample, probably as a consequence of the formation of weaker and/or less organized SM crystalline domains due to the previously discussed factors.

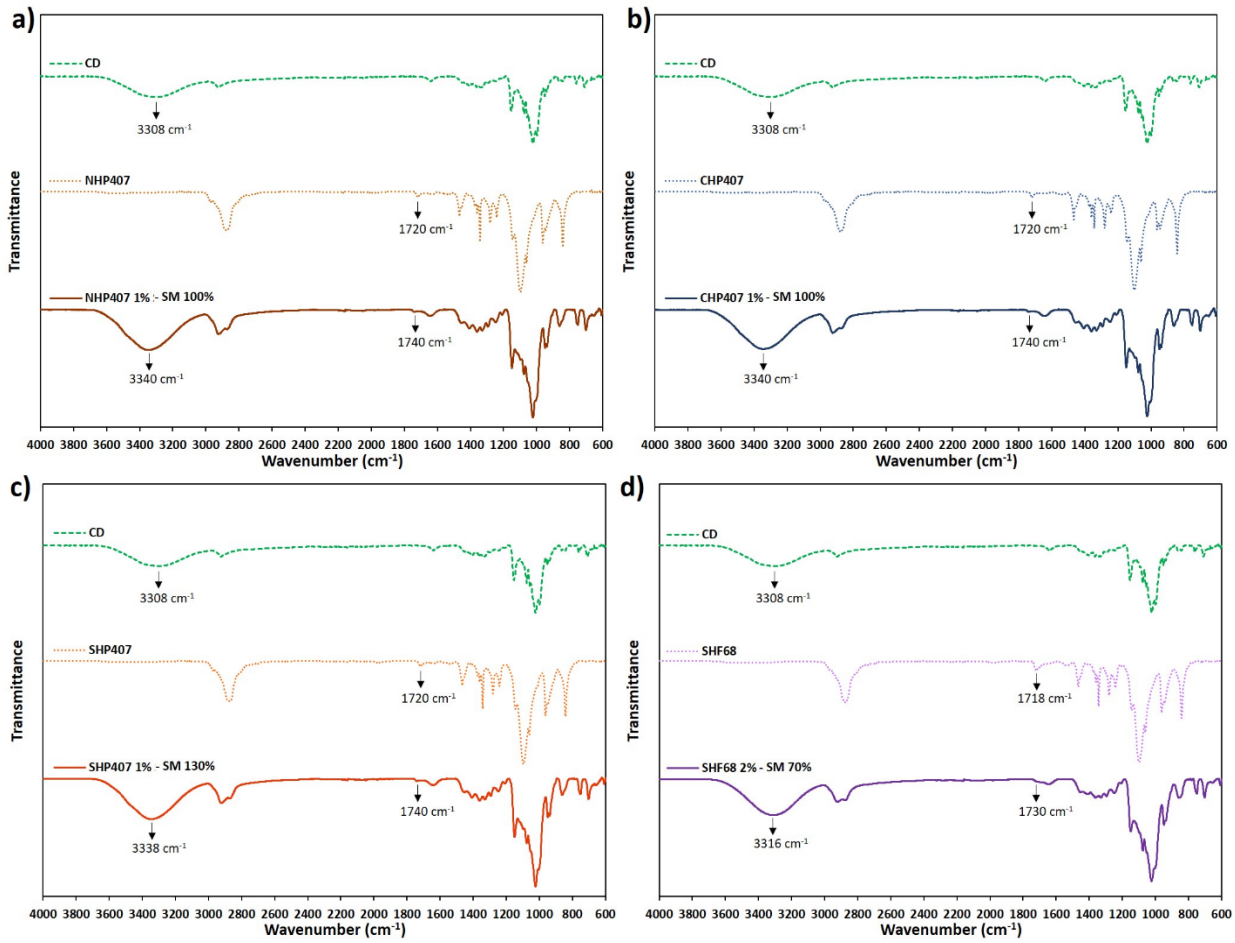


Figure 4: *ATR-FTIR spectra of CDs (dashed lines, green), pure PEUs (dotted lines) and SM crystalline powders (continuous lines) of a) NHP407 (brown), b) CHP407 (blue), c) SHP407 (orange), and d) SHF68 (purple). All the peaks subjected to significant shifts are indicated with black arrows.*

3.2.3 ^{1}H-NMR spectroscopic analyses of SM structures

The co-presence of PEUs and CDs in the crystalline matter derived from the mixture of the two components in ddH_2O was further assessed through ^{1}H-NMR spectroscopic characterization that was performed on the same samples used for XRD crystallography and ATR-FTIR spectroscopy after complete re-solubilization in D_2O (figure S3 of supplementary material). The presence of the resonances at 3.63 ppm and in the region between 1.5 and 0.9 ppm proved PEU involvement in the formation of SM crystals, while the peaks in the range from 4.0 to 3.7 ppm, from 3.55 to 3.45 ppm and at 5.07 ppm were originated by the presence of CDs. The correlation between XRD crystallography, ATR-FTIR and ^{1}H-NMR spectroscopies represented a set of proofs demonstrating the successful formation of PPR-based SM crystals based on PEUs. Nonetheless,

the relevant complexity of the resulting systems was a hindering element for the determination of more specific parameters, such as constants of association between the two components.

On the basis of all the previous physico-chemical characterizations, a qualitative representation of the physical arrangement involving PEU chains and CDs into a supramolecular network is reported in figure S4 of supplementary material.

3.3 Supramolecular hydrogel characterization

3.3.1 SM hydrogel formulation and gelation kinetics

PEU and CD solutions showing the potentiality to form gelling systems (i.e., PEU concentration ranging from 1% to 5% w/v and CDs at 10% w/v) were selected according to our previous studies.[63] The composition and the gelation time of the investigated hydrogel formulations are reported in table 3 according to the representation proposed by Ahmad *et al.* with slight modifications.[84]

Hydrogel formulation	CHP407 (mg ml^{-1})	NHP407 (mg ml^{-1})	SHP407 (mg ml^{-1})	NHF68 (mg ml^{-1})	SHF68 (mg ml^{-1})	CDs (mg ml^{-1})	Gelation time
CHP407 1% - CD 10%	10	-	-	-	-	100	O.N.
CHP407 3% - CD 10%	30	-	-	-	-	100	2 h 20 min
CHP407 5% - CD 10%	50	-	-	-	-	100	1 h 30 min
NHP407 1% - CD 10%	-	10	-	-	-	100	O.N.
NHP407 3% - CD 10%	-	30	-	-	-	100	2 h 20 min
NHP407 5% - CD 10%	-	50	-	-	-	100	2 h 30 min
SHP407 1% - CD 10%	-	-	10	-	-	100	O.N.
SHP407 3% - CD 10%	-	-	30	-	-	100	3 h
SHP407 5% - CD 10%	-	-	50	-	-	100	2 h
BLEND 1% - CD 10%	8	-	-	-	2	100	O.N.
BLEND 3% - CD 10%	24	-	-	-	6	100	2 h 20 min
BLEND 5% - CD 10%	40	-	-	-	10	100	1h
NHF68 1% - CD 10%	-	-	-	10	-	100	SOL
NHF68 3% - CD 10%	-	-	-	30	-	100	72 h
NHF68 5% - CD 10%	-	-	-	50	-	100	72 h
SHF68 1% - CD 10%	-	-	-	-	10	100	O.N.
SHF68 3% - CD 10%	-	-	-	-	30	100	O.N.
SHF68 5% - CD 10%	-	-	-	-	50	100	5h 30 min

Table 3: *Composition and gelation time of the investigated hydrogel formulations. Gelation time was estimated at room temperature (i.e. 25 °C) through tube inverting test.*

NHF68-based samples were characterized by non-gelling conditions (i.e., NHF68 at 1% w/v) or significantly slower gelation kinetics with respect to all the other formulations (at 3% and 5% w/v), in accordance with the previous considerations in section 3.2. For these relevant physico-chemical limitations, NHF68 was not selected for further characterizations and applications. Similarly, SHF68-based hydrogels required longer incubation times to observe the formation of stable and solid gels with respect to P407-based systems. Nevertheless, SHF68 samples exhibited still acceptable gelation kinetics compared to NHF68 systems and its polymer chains exposed a remarkable amount of free primary amines, which could be exploited for further functionalization procedures or to provide gels with a pH-responsive behavior. For this reason, SHF68 was maintained in the formulation of blends with CHP407 (i.e., BLENDS, composed of SHF68 at 20% wt/wt and CHP407 at 80% wt/wt), which did not show any specific chemical functionality. The combination of these two PEUs characterized by a similar chemical structure, but different properties (e.g., PPO content, molar mass) resulted in formulations with interesting behaviors. For instance, the sample BLEND 5% - CD 10% showed faster gelation kinetics with respect to the other samples at the same PEU concentration (i.e., 5% w/v). This improved gelation kinetics could result from the onset of constructive interactions between CHP407 and SHF68 chains, which favored the formation of a more interconnected hydrogel network. Indeed, shorter and more soluble SHF68 chains were probably involved in the formation of physical links and/or entanglements with the more structured CHP407-based aggregates.[85–87] Pure CHP407-based gels showed faster gelation kinetics compared to other formulations due to the absence of any pendant group and a composition characterized by various hydrophobic domains (i.e., PPO, HDI and CDM). Interestingly, the hydrogel based on SHP407 at 5% w/v showed faster gelation with respect to the system composed of NHP407 at the same concentration. The reason for this difference could be found in the different interaction of NHP407 and SHP407 chains with PBS anions in solution. Indeed, the free primary amines of SHP407 probably interact with polar domains of phosphate salts,[87] thus inducing a stabilizing effect on the polymer network to enhance cyclodextrin threading along polymer chains. This behavior is in accordance with the previously discussed results from CMT characterization, in which SHP407 showed a slightly lower CMT in PBS compared to ddH_2O. A similar behavior could be supposed also for systems based on SHF68 that showed a relatively higher number of free amines (i.e., approx. 6-fold greater than SHP407) compared to SHP407. Interestingly, differences in gelation timing between NHP407- and SHP407-based hydrogels at 3% w/v PEU concentration followed an opposite trend with respect to the systems designed at higher PEU contents (i.e., 5% w/v). Indeed, the hydrogel system composed of NHP407 at 3% w/v concentration showed a faster gelation kinetics with

respect to the one based on SHP407 at equal concentration. Such surprising behavior could be dependent on highly complex physical and intermolecular interactions (e.g., entanglements, hydrophobic interactions, hydrogen bonds, salting-out effect, and steric hindrance), which influenced the SM self-assembly in a non-linear manner. Hence, at lower PEU concentration, i.e., lower PEU/CD ratio, the additional contribution of Boc groups as hydrophobic domains probably plays a more evident role in determining gelation kinetics, rather than the presence of free primary amines. Indeed, in agreement with our previous considerations concerning physico-chemical characterizations (i.e., XRD crystallography and ATR-FTIR spectroscopy), in such conditions the presence of Boc groups most likely stabilizes the PEU-based networks, while at higher PEU/CD mass ratio (i.e., higher PEU content, 5% w/v) Boc domains probably hinder the mobility of the network and a better balance could be identified in a more linear structure showing polar domains as in SHP407. Based on gelation time results, CHP407-, SHP407- and BLEND-based systems were selected for further characterizations.

3.3.2 SM hydrogel rheological characterization

Rheological characterizations provided information on the physical behavior of hydrogels in terms of mechanical properties, which in turn determine the general processability of hydrogel systems and their potential applications. The extreme values of the investigated range of PEU concentrations were selected for all rheological studies (i.e., 1 and 5% w/v). Frequency sweep tests were performed at three different temperatures (25, 30 and 37 °C) with the aim to assess the degree of gel development of SM systems, since all PEUs showed a thermo-responsive behavior (Figure 5). Irrespective of temperature, all formulations were characterized by the typical mechanical response of fully developed gels. Indeed, at every temperature the storage modulus (G') was greater than the loss one (G") throughout the entire range of analyzed frequencies and independent over frequency. Moreover, the mechanical properties improved by increasing temperature, thus indicating a thermo-thickening response of SM hydrogels (e.g., G' at 100 rad s^{-1} for CHP407 1% - CD 10% resulted to be 3620 Pa and 5820 Pa at 25 and 37 °C, respectively). CHP407-based systems showed the highest values of G' and G", while SHP407-based hydrogels the lowest ones. The systems based on the blends of CHP407 and SHF68 were characterized by intermediate mechanical properties. These results, in addition to all previous considerations regarding the formation of SM complexes (i.e., XRD crystallography and ATR-FTIR spectroscopy) led to the election of CHP407 as the best PEU interacting with CDs at the SM level. CHP407 high hydrophobicity and absence of pendant moieties along its backbone most likely enhanced CD threading along its chains and the crystallization process of formed PPRs. The lower mechanical

properties of CHP407/SHF68 blends could be correlated with the lower content in hydrophobic domains and the weak interaction of SHF68 with CDs. Indeed, SHF68 might predominantly act as stabilization agent of CHP407 micelles and aggregates, thus inducing a faster SM gelation process through CHP407 chains with no improvement in storage and loss moduli.

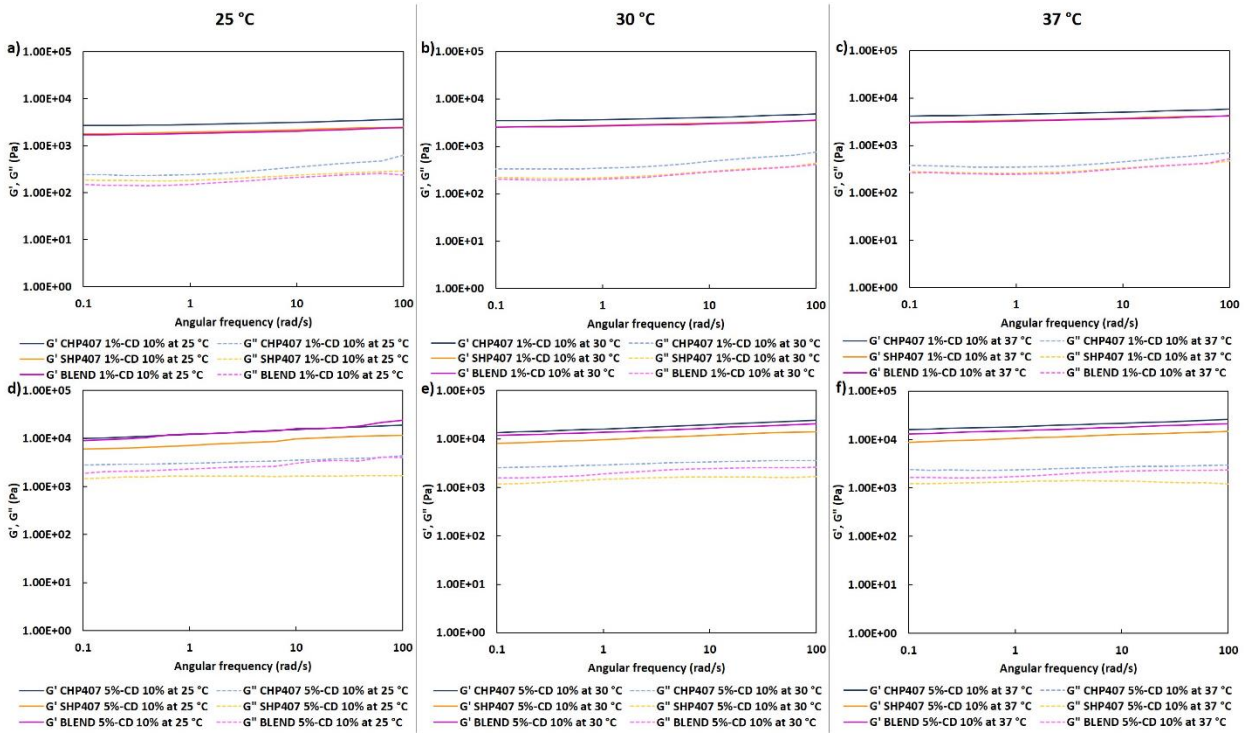


Figure 5: *G' (continuous line) and G" (dashed line) trends as a function of angular frequency measured at three different temperatures: a) and d) at 25 °C, b) and e) at 30 °C, c) and f) at 37 °C for hydrogels based on CHP407 (blue), SHP407 (orange) and BLEND (purple).*

Strain sweep tests were performed to define the linear viscoelastic region (LVE) and deformation at break (γ_L) of hydrogels to applied strain. Hydrogels were tested up to a total strain of 500% and then the same protocol was repeated after 15 minutes of recovery at 37 °C to evaluate sample self-healing ability upon application of remarkable deformations. Figure 6 reports the recorded curves. As summarized in Table 4, an elastic modulus recovery greater than 83% was observed for all formulations, thus indicating noteworthy self-healing abilities. CHP407-based hydrogels showed the highest storage and loss moduli values within the LVE (G'_{LVE} and $G"_{LVE}$, respectively), but lower strains before complete rupture (γ_L). This could be explained by the higher degree of SM crystallization of PPRs that conferred higher stiffness and fragility to the resulting networks. SHP407- and BLEND-based systems showed comparable responses, but for higher concentrations (5% w/v) the latter showed better mechanical properties, being mainly composed

of CHP407 and due to the toughening effect of SHF68 on the resulting network. No clear dependence of γ_L over the recovery process was observed. Nonetheless, samples containing PEU at 1% w/v concentration were negatively affected by the rupture process, since the values of γ_L upon recovery ($\gamma_{L_recovery}$) resulted to decrease for all PEU formulations, while no significant variations were observed for samples at 5% w/v PEU concentration. This different outcome can be probably ascribed to the lower amount of free PEU domains and hence to a marked SM and crystalline character of the resulting hydrogel network in samples at 1% w/v PEU concentration, as hypothesized in our previous investigations.[63]

	G'_{LVE} (Pa)	G''_{LVE} (Pa)	G'_{LVE} recovered (%)	γ_L (%)	$\gamma_{L_recovery}$ (%)
CHP407 1% - CD 10%	4500	350	91	0.29	0.13
CHP407 5% - CD 10%	15400	2300	87	0.29	0.50
SHP407 1% - CD 10%	4000	240	88	1.00	0.45
SHP407 5% - CD 10%	10000	1400	91	0.48	0.56
BLEND 1% - CD 10%	3600	280	97	0.70	0.38
BLEND 5% - CD 10%	14700	1500	83	0.55	0.50

Table 4: *Summary of strain sweep test main parameters: G'_{LVE} (storage modulus within LVE), G''_{LVE} (loss modulus within LVE), G'_{LVE} recovered (%) (percentage of G'_{LVE} recovered after 15 minutes of sample quiescence at 37 °C), γ_L (strain at which the network rupture occurs), $\gamma_{L_recovery}$ (strain at which the rupture occurs by repeating the test after 15 minutes of recovery at 37 °C).*

Time dependent strain tests were performed by applying a 0.1% strain for 120 seconds and then by immediately increasing it to 100% for 60 seconds. This procedure was repeated three times and then the starting deformation was applied again in order to quantify the general recovery after cyclic stress. Figure 6 reports the trends of G' and G'' as a function of time during application of the previously described procedure. During the rupture phases, G' reached significantly lower values than G", indicating a transition from a completely developed gel to a viscoelastic fluid characterized by neglectable storage modulus values with respect to loss ones. Once the recovery phase was applied again, the gel state was stabilized again within 30 seconds in all the formulations. After 3 complete rupture cycles, the recovery of G' was greater than 84% with respect to the initial value for all the analyzed hydrogels, as indicated in Table 5. SHP407-based hydrogel at 5% w/v polymer concentration completely recovered G', probably for its less developed SM network composed of PPR-based crystals that resulted in an enhanced reversibility, in which the role of PEU chains resulted to be highly effective. A similar behavior was observed in BLEND samples in which the presence of SHF68 was responsible for a higher G' recovery than the one observed for hydrogels based on pure CHP407. These results highlighted

hydrogel remarkable mechanical properties characterized by self-healing and thixotropic behaviors even for formulations with very low PEU concentration (1% w/v).

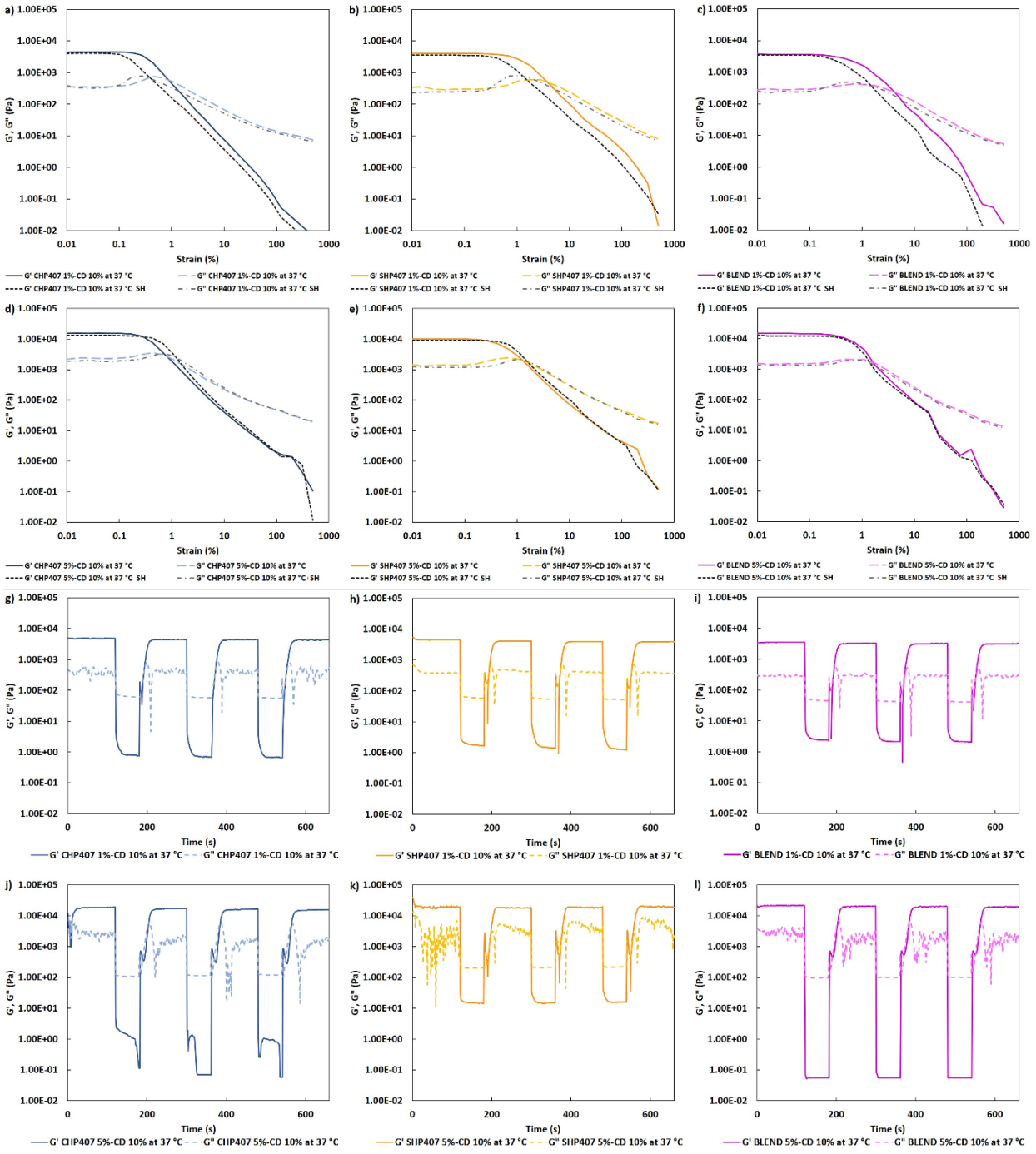


Figure 6: *G' (continuous line) and G" (dashed line) trends as a function of applied strain for CHP407 (blue, a) 1% w/v, d) 5% w/v), SHP407 (orange, b) 1% w/v, e) 5% w/v) and BLEND (purple, c) 1% w/v, f) 5% w/v) hydrogels. G' (black short-dashed line) and G" (grey dash-dotted line) after self-healing (15 minutes at 37 °C) are also reported. Self-healing test curves representing G' (continuous line) and G" (dashed line) as a function of time for CHP407 (blue, g) 1% w/v, j) 5% w/v), SHP407 (orange, h) 1% w/v, k) 5% w/v) and BLEND (purple, i) 1% w/v, l) 5%*

w/v) hydrogels during application of cyclic stress. Recovery phases (0.1 % strain) are characterized by G'>G", while rupture phases (100 % strain) are determined by G">G', thus indicating a complete hydrogel rupture and a thixotropic response.

	G' recovered (%) after 3 cyclic ruptures
CHP407 1% - CD 10%	89
CHP407 5% - CD 10%	84
SHP407 1% - CD 10%	88
SHP407 5% - CD 10%	100
BLEND 1% - CD 10%	90
BLEND 5% - CD 10%	92

Table 5: *Percentage of G' recovery (G' recovered (%)) after 3 rupture cycles at 100% strain. Recovery was evaluated with respect to starting G' values.*

From a general perspective, the results obtained through rheological characterizations indicated well-developed, mechanically stable, and highly self-healing physical hydrogels formulated at low polymeric content (i.e., ≤ 5% w/v). Moreover, these properties turned out to be tunable depending on the chemical features of the PEUs. The combination of these properties represents a notable achievement with respect to the state of the art concerning the development of supramolecular hydrogels for drug delivery. In fact, even in very recent and notable studies, similar mechanical features were reached at remarkably higher concentration (>10% w/v) of commercially available polymers, such as PEO and Pluronics®.[88–90] Other examples showed similar mechanical and physical properties for hydrogels based on copolymers composed of PEO and PLA.[54] However, a limited physico-chemical tunability can be appreciated in these cases for the resulting supramolecular hydrogels with respect to PEU-based ones, as deeply documented with the above-discussed results.

3.3.3 Swelling and stability of SM hydrogels in watery environment

Swelling and stability tests were performed to study hydrogel behavior in contact with a watery environment. In detail, swelling tests describe the response of hydrogels in terms of water absorption, while stability tests refer to the dissolution of polymeric or other constituting components of hydrogel networks. The equilibrium between these two aspects can be summarized through the calculation of swelling ratio values. Nevertheless, only the entire set of these correlated characterizations can thoroughly describe the behavior of physically crosslinked hydrogels in contact with watery environments, since these systems could show the ability to

absorb a high amount of water while releasing a significant mass of constituting molecules. In detail, swelling and stability test results are shown figure 7. From a general perspective, the total duration of hydrogels in contact with refreshed aqueous external medium was comparable to the one observed for similar systems.[55,58,91] SM hydrogels did not show significant swelling by increasing their wet mass. However, a simultaneous and prominent release of hydrogel components was measured. This behavior could be explained as a continuous and balanced mass exchange with the external environment by absorbing water and releasing less stable entities, such as free CDs and PEU chains/aggregates. Once all instable components were released, the complete dissolution of the hydrogels occurred within the next time step. Interestingly, SM hydrogels with a PEU concentration of 1% w/v showed a lower tendency to de-swell with respect to the formulations at 3 and 5% w/v PEU concentrations. Simultaneously, these samples showed a significantly higher release of their constituents with respect to their total dry mass. This peculiar behavior was translated in the ability of the SM systems to maintain their shape, while strongly interacting with the surrounding water-based milieu. As a confirmation of this, the measured swelling ratios of samples containing PEU at 1% w/v concentration were significantly higher than the ones obtained for other formulations (figure 7).

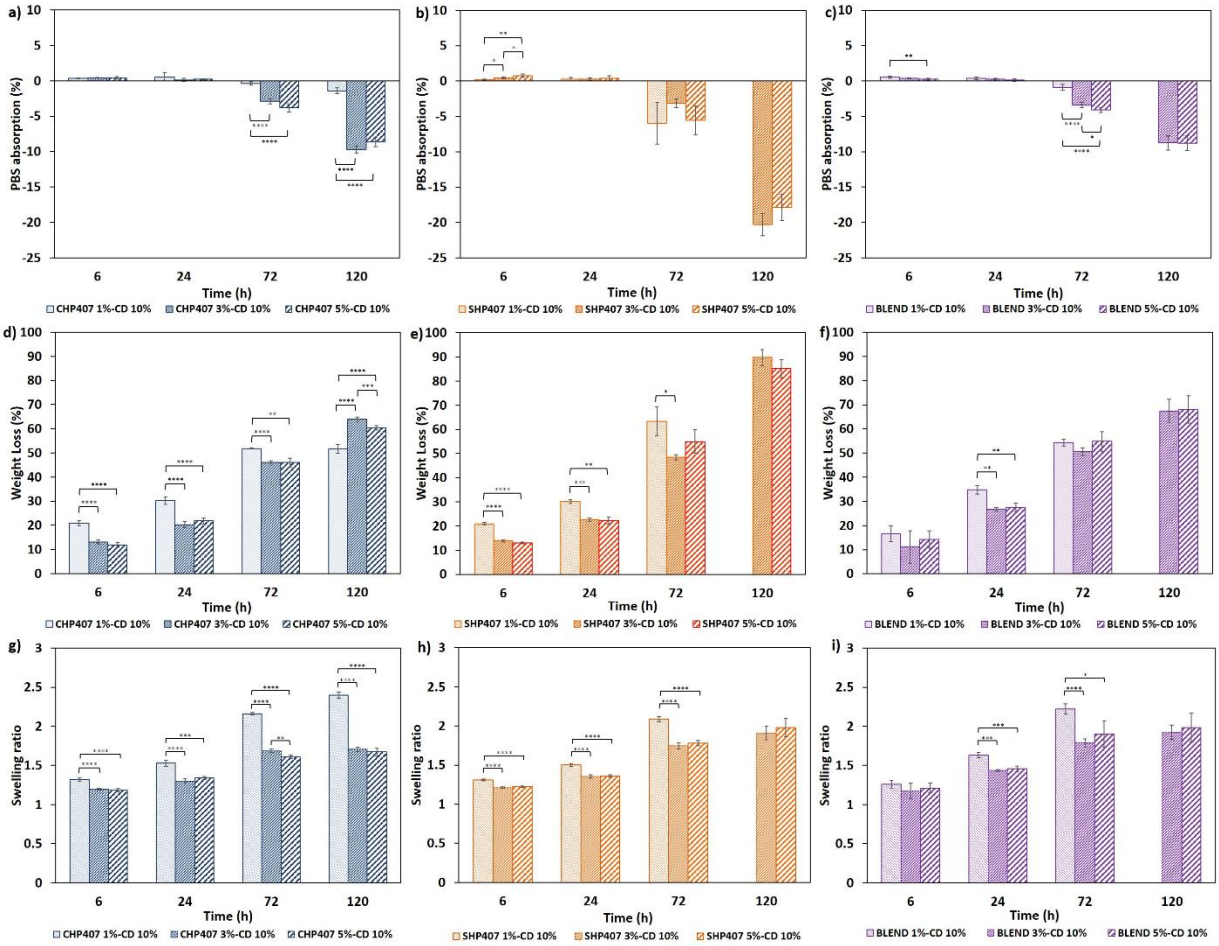


Figure 7: *PBS absorption (%) and weight loss (%) bar diagrams for CHP407 (blue, a) and d)), SHP407 (orange, b) and e)) and BLEND (purple, c) and f)) hydrogels. Swelling ratio bar diagrams for CHP407 (blue, g)), SHP407 (orange, h)) and BLEND (purple, i)) hydrogels.*

This result could suggest that the hydrogel network which characterizes samples at 1% w/v PEU concentration was determined by a marked supramolecular character. Indeed, the polymeric counterpart of such systems was mainly based on simple structures (i.e., micelles or small micelle aggregates), which exhibited fewer constraints (e.g., micelle-based supramolecular aggregates, entanglement) hindering the interaction with CDs. Hence, the pronounced supramolecular character in terms of PPR crystals of these systems probably provided them with a more responsive and remarkably stable behavior. However, although samples at higher PEU concentrations showed good response and stability in watery environment, in absolute terms they released the highest amount of polymeric structures, with no significant differences between hydrogels containing PEUs at 3% and 5% w/v concentration. This datum may indicate that at the same CD concentration a higher amount of PEU in the samples resulted in hydrogel networks in

which a fraction of polymer was not involved in the formation of stable SM crystals. As a consequence, such purely polymeric structures were more inclined to be solubilized and released in the eluates. SHP407 hydrogels showed the highest rate of dissolution probably because of its higher solubility derived from the presence of lateral domains (i.e., primary amines) that could enhance chain interaction with water. For this reason, SHP407 hydrogels appeared as the weakest in terms of stability, but the best in terms of responsiveness. This result was completely in accordance with the higher reversibility obtained through rheological characterizations. No significant differences in PBS absorption were generally found between CHP407- and BLEND-based hydrogels, while slightly but significantly higher dissolution rates of BLEND samples were measured (data not shown) at 24 hours (p-value = 0.0043 for BLEND 1%-CD 10% and CHP407 1%-CD 10%; p-value = 0.025 for BLEND 3%-CD 10% and CHP407 3%-CD 10%). On the contrary, significantly higher swelling ratios were recorded for BLEND samples with respect to CHP407 hydrogels at different time steps (e.g., at 24 hours, p-value = 0.048, 0.0039 and 0.0084 at 1, 3 and 5% w/v polymer concentration, respectively). This result was a general indication for a higher responsiveness of BLEND samples with respect to CHP407 hydrogels. Nonetheless, for prolonged time frames CHP407-based hydrogels at low PEU concentration showed an improved stability with respect to other PEU-based hydrogels with the same composition (after an incubation time of 5 days, CHP407 1%-CD 10% showed a partial weight loss of 51.6 ± 1.7%, while the comparable systems based on SHP407 and BLEND were completely dissolved). This behavior resulted to be in complete accordance with rheological characterizations, in which CHP407-based hydrogels showed the best network arrangement thanks to a balanced integration of hydrophobic interactions and crystallization of PPRs.

To summarize, swelling and stability test results evidenced a hydrogel behavior particularly suitable for drug delivery applications. Indeed, all the formulated systems were able to release a great amount of drug carriers, such as free CDs, CD clusters and PEU aggregates, through a bulk-erosion mechanism that preserved the integrity of hydrogel shape. The fact these results were achieved at remarkably low concentrations of PEUs highlighted the suitability of such properly synthesized polymers as building blocks of functional and tunable hydrogels for drug delivery. Indeed, this feature decreases the risk of local and/or systemic toxicity due to the relevant release of amphiphilic polymer chains [62].

3.3.4 Cytotoxicity evaluation

Cytotoxicity was evaluated on formulations containing exclusively SHP407, CHP407 or SHF68 in order to assess potential side effects separately. All SM hydrogels did not show any cytotoxic behavior, with cell viability around 100%, as shown in figure S5 of supplementary material. In order to minimize the content of synthetic polymer and based on previous considerations on SM gel stability and responsiveness in watery environment, formulations with PEU concentrations of 1% and 3% w/v were selected for further investigations as curcumin carriers.

3.4 Curcumin encapsulation and characterization of curcumin-loaded hydrogels

3.4.1 Rheological characterization of curcumin-loaded SM hydrogels

The effects of solvent composition and Cur encapsulation on SM hydrogel (1% w/v) properties were evaluated through rheological characterizations (i.e., strain sweep, frequency sweep and self-healing tests). Three conditions were compared in order to separate single effects that might induce any variation on hydrogel mechanical response. The obtained results are collected in figure S6 and S7 of supplementary material file. From a general perspective, the typical "gel" state of the investigated formulations was preserved in all the tested conditions and the major contribution to the variation of SM hydrogel properties could be ascribed to the presence of a fraction of water into the system rather than to Cur encapsulation. Indeed, it is likely that a weaker salting-out effect occurred in the formulations containing ddH_2O (i.e., samples coded as PEU 1%-CD 10%-PBS/H_2O), in accordance with the previously discussed results obtained from the characterization of CMTs of PEUs in PBS and ddH_2O solutions. CHP407- and BLEND-based samples prepared in the mixture PBS/ddH_2O showed the greatest decrease in mechanical properties. Indeed, their G' value at 100 rad s^{-1} and 37 °C decreased approx. 45% compared to samples prepared in pure PBS, while hydrogels composed of SHP407 showed a decrement of circa 35% in the same conditions. The highly crystalline SM network of CHP407- and BLEND-based hydrogels was probably more affected by solvent composition with respect to the less crystalline system deriving from SHP407. Moreover, in all hydrogel systems the additional presence of Cur generally resulted in a tendency to maintain better mechanical properties with respect to control samples (i.e., samples prepared in the mixture of PBS and ddH_2O). This behavior could be correlated to the possibility of supplementary interactions between Cur and the hydrophobic domains of PEU chains. The presence of ddH_2O or even Cur did not exert a detrimental contribution on the reversibility (i.e., self-healing ability) of the resulting hydrogels, as reported in figure S7, which contains the data obtained from strain sweep and self-healing tests.

In accordance with the characterizations based on frequency sweep tests, the effects of both solvent composition and the additional presence of Cur prevalently influenced the entity of mechanical properties (i.e., G' and G"), while hydrogel responsiveness and reversibility were not significantly modulated in relative terms.

3.4.2 Release studies of curcumin

Delivery profiles ~~studies~~ of curcumin from SM hydrogels at 37 °C are reported in figure 8 (mass of released curcumin *vs.* time) and figure S8 of supplementary material (values as percentages of the theoretical payload (80 μg ml^{-1},100%)), showing remarkably progressive release kinetics, as well as the absence of any initial burst release. Indeed, within the first six hours of observation, release curves were characterized by a gradual and approximately linear trend. The formulations containing PEUs at 1% w/v concentration showed significantly higher payload release (approx. two-fold) with respect to the samples at 3% w/v concentration during the first 6 hours of incubation. This behavior could be explained by referring to swelling and stability data: samples at 1% w/v PEU concentration were characterized by enhanced release of free hydrogel components and hence greater swelling ratio, thus permitting a general curcumin mass release approximately two-fold higher than the samples with 3% w/v polymer concentration. From this point of view, considering the general therapeutic local concentration of curcumin for most applications (i.e., micromolar), the observed pharmacokinetics could induce different effects in terms of neoplastic cell growth or lytic cytokine secretion inhibition.[18,72,92]

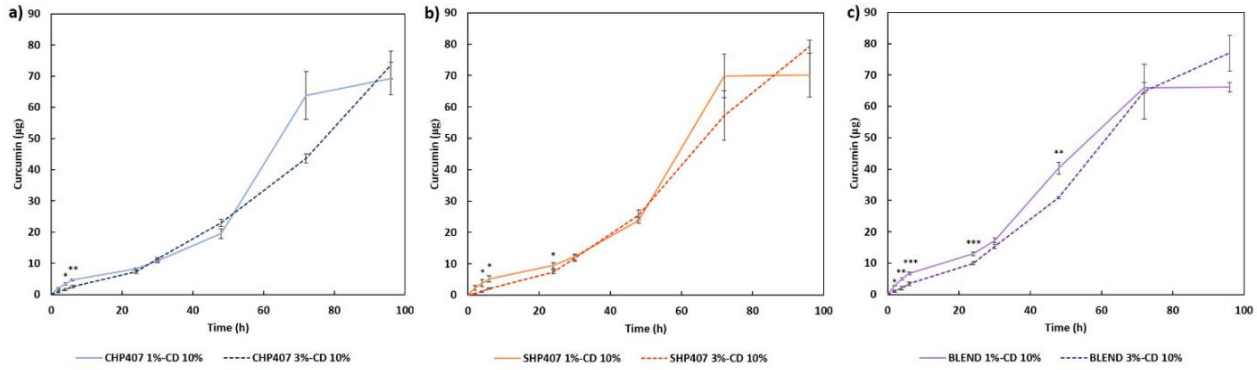


Figure 8: *Cur release profiles for CHP407 (a, blue), SHP407 (b, orange) and BLEND (c, purple) hydrogels. In each graph, 1% (continuous lines) and 3% (dashed lines) w/v PEU concentrations are compared.*

In addition, the Peppas release exponent was calculated within the first 6 hours of Cur release and the obtained values were in the range between 0.7 and 0.89 for the samples containing PEU

at 1% w/v concentration, indicating a release mechanism based on mixed swelling and diffusion (anomalous transport) of the encapsulated drug. Differently, the samples at 3% w/v PEU content were characterized by exponents greater than 0.89, thus suggesting a super Case II model, in which the transport of the drug is extremized by the induction of mechanical tensions into hydrogel network due to a relevant mass exchange. This different behavior can be ascribed to the higher stiffness of 3% w/v concentrated SM hydrogels with respect to the samples formulated at 1% w/v concentration. Indeed, the presence of a higher PEU content could be responsible of the formation of a tighter hydrogel network, which could be more susceptible to tension formation. Within the previously commented trends, CHP407 3%-CD 10% sample turned out to be an exception with its *n* value equal to 0.82. The reason for this different output could be found in the enhanced responsiveness and then higher instability of SHP407 and BLEND samples, as previously discussed. In fact, the hydrogel behavior configured with a super Case II model could be correlated with the higher velocity of solvent absorption caused by the presence of water-attractive elements (i.e., free amines) and hence the marked release of hydrogel structures, in addition to the intrinsic lower stability due to the weaker formation of crystallized PPRs. Finally, after 48 hours of observation, an acceleration in Cur release was observed in all the studied samples. In fact, a relatively high rate of Cur release was measured for all the formulations also during the incubation step between 3 and 4 days (i.e., the release kinetics did not show a plateau). This can be ascribed to the progressive bulk and surface erosion of the physical hydrogel network that allowed the delivery of such hydrophobic drug, leading to complete hydrogel dissolution at 96 hours. The slight tendence of the hydrogels containing PEUs at 1% w/v to decrease the final release rate with respect to samples containing PEUs at 3% w/v could be related to their more pronounced supramolecular character due to a lower PEU/CD ratio, as widely discussed in the paragraph concerning swelling and stability tests (paragraph 3.3.3). Nonetheless, the differences between the systems containing PEU at 1% and 3% w/v immediately before complete solubilization (i.e., between 3 and 4 days incubation) were not significant.

4. Conclusions

In this work, a library of different PEUs has been developed and thoroughly characterized. In detail, two different PEO-PPO-PEO triblock copolymers were selected for PEU production due to their interesting tendency to form PPR-based SM hydrogels.[79] The other reagents (HDI, CDM and NBoc) were chosen with the aim to tune the final properties and open the way to the possibility to further functionalize the resulting polymers. Interestingly, the synthesized PEUs showed different affinities with CDs. Indeed, due to the *LEGO*-like structure of PEUs, their behavior in

aqueous solution resulted in more complex dynamics than Poloxamer/Pluronic as such, which could be correlated with the occurrence of specific inter-polymer interactions. For these reasons, we hypothesized that PPO and other hydrophobic domains (i.e., CDM and HDI) within PEU backbone play a fundamental role in network stabilization and CD threading enhancement when molar mass reaches relatively high values.

PEU-based SM hydrogels were then formulated at CD concentration of 10% w/v and notably low polymeric content ranging between concentrations of 1 and 5% w/v. The mechanical properties and the responsiveness of the developed hydrogels in watery environments were strictly correlated to PEU chemical features, which can be easily modified according to a simple synthesis procedure and subsequent functionalization. Linear, hydrophobic, and rigid polymer structures (i.e., CHP407) conferred better mechanical properties (greater values of storage modulus) and enhanced stability in contact with watery environment to the supramolecular hydrogels. Differently, the presence of pendant primary amines along PEU chains (SHP407 and BLEND systems) enhanced the mechanical reversibility (i.e., self-healing) and the responsiveness of the supramolecular networks. These findings represent an important set of information to design and engineer polymeric molecules for the development of effective supramolecular hydrogels.

In addition, the concomitant use of cyclodextrins allows both the self-assembly of hydrogel network and drug encapsulation at high dosages. Hence, the combination of α-cyclodextrins and thermosensitive nanostructures (i.e., micelles) based on custom-made PEUs was exploited for the stabilization, preservation, and subsequent controlled release of curcumin as therapeutic agent and model molecule of highly hydrophobic drugs, which are generally affected by limited bioavailability *in vivo*.

Therefore, this study highlighted the noteworthy tunability and versatility of the here-developed and characterized plethora of PEU-based SM systems, which represent an ensemble of promising injectable formulations to easily deposit and progressively deliver *in loco* extremely low bioavailable molecules, such as curcumin. Moreover, the remarkable reversibility of these systems could allow an easy integration with other nanotechnologies, such as stimuli-sensitive drug-loaded nanoparticles for multiple therapeutic and diagnostic (i.e., theranostic) purposes.[67,93,94] Finally, for all the above-mentioned properties, these PEU-based supramolecular hydrogels could provide a significant contribution of improvement for challenging and unmet clinical needs.

Supplementary Material

Detailed figure containing ATR-FTIR spectra of synthesized PEUs (S1); additional figure containing CMT curves of PEU-based solutions in bi-distilled water (S2); figure containing ^{1}H-NMR spectra of dissolved crystals based on poly(pseudo)rotaxanes (S3); figure showing a qualitative representation of the physical arrangement of PEUs and CDs into supramolecular networks (S4); figure reporting the results of cytotoxicity tests (S5); figure showing frequency sweep tests of SM hydrogels composed of various media (PBS, ddH_2O/PBS mixture) and containing Cur (80 µg ml^{-1}) at various temperatures (i.e., 25, 30 and 37 °C) (S6); figure containing strain sweep and self-healing tests of SM hydrogels composed of various media (PBS, ddH_2O/PBS mixture) and loaded with Cur (80 µg ml^{-1}) at 37 °C (S7); figure representing the trends of curcumin release as percentage of the theoretical payload (80 µg ml-1, 100%) *vs.* time (S8).

References

[1] T. Loftsson, M.E. Brewster, Pharmaceutical applications of cyclodextrins: basic science and product development: Pharmaceutical applications of cyclodextrins, Journal of Pharmacy and Pharmacology. 62 (2010) 1607–1621. https://doi.org/10.1111/j.2042-7158.2010.01030.x.

[2] N. Sharma, A. Baldi, Exploring versatile applications of cyclodextrins: an overview, Drug Delivery. 23 (2016) 729–747. https://doi.org/10.3109/10717544.2014.938839.

[3] G. Liu, Q. Yuan, G. Hollett, W. Zhao, Y. Kang, J. Wu, Cyclodextrin-based host–guest supramolecular hydrogel and its application in biomedical fields, Polym. Chem. 9 (2018) 3436–3449. https://doi.org/10.1039/C8PY00730F.

[4] V. Parmar, G. Patel, N.Y. Abu-Thabit, Responsive cyclodextrins as polymeric carriers for drug delivery applications, in: Stimuli Responsive Polymeric Nanocarriers for Drug Delivery Applications, Volume 1, Elsevier, 2018: pp. 555–580. https://doi.org/10.1016/B978-0-08-101997-9.00024-2.

[5] É. Fenyvesi, M. Vikmon, L. Szente, Cyclodextrins in Food Technology and Human Nutrition: Benefits and Limitations, Critical Reviews in Food Science and Nutrition. 56 (2016) 1981–2004. https://doi.org/10.1080/10408398.2013.809513.

[6] A.A. Karim, X.J. Loh, CHAPTER 9. Towards Cyclodextrin-Based Supramolecular Materials, in: X.J. Loh (Ed.), Polymer Chemistry Series, Royal Society of Chemistry, Cambridge, 2016: pp. 154–177. https://doi.org/10.1039/9781782623984-00154.

[7] É. Euvrard, N. Morin-Crini, C. Druart, J. Bugnet, B. Martel, C. Cosentino, V. Moutarlier, G. Crini, Cross-linked cyclodextrin-based material for treatment of metals and organic substances present in industrial discharge waters, Beilstein J. Org. Chem. 12 (2016) 1826–1838. https://doi.org/10.3762/bjoc.12.172.

[8] P. Jansook, S.V. Kurkov, T. Loftsson, Cyclodextrins as solubilizers: Formation of complex aggregates, Journal of Pharmaceutical Sciences. 99 (2010) 719–729. https://doi.org/10.1002/jps.21861.

[9] Á. Haimhoffer, Á. Rusznyák, K. Réti-Nagy, G. Vasvári, J. Váradi, M. Vecsernyés, I. Bácskay, P. Fehér, Z. Ujhelyi, F. Fenyvesi, Cyclodextrins in Drug Delivery Systems and Their Effects on Biological Barriers, Sci. Pharm. 87 (2019) 33. https://doi.org/10.3390/scipharm87040033.
[10] S.A. Nepogodiev, J.F. Stoddart, Cyclodextrin-Based Catenanes and Rotaxanes †, Chem. Rev. 98 (1998) 1959–1976. https://doi.org/10.1021/cr970049w.
[11] X. Ma, Y. Zhao, Biomedical Applications of Supramolecular Systems Based on Host–Guest Interactions, Chem. Rev. 115 (2015) 7794–7839. https://doi.org/10.1021/cr500392w.
[12] T. Loftsson, D. Hreinsdóttir, M. Másson, Evaluation of cyclodextrin solubilization of drugs, International Journal of Pharmaceutics. 302 (2005) 18–28. https://doi.org/10.1016/j.ijpharm.2005.05.042.
[13] Z.H. Qi, V. Mak, L. Diaz, D.M. Grant, C.J. Chang, Molecular recognition: .alpha.-cyclodextrin and penicillin V inclusion complexation, J. Org. Chem. 56 (1991) 1537–1542. https://doi.org/10.1021/jo00004a037.
[14] T. Loftsson, B.J. Ólafsdóttir, Cyclodextrin-accelerated degradation of β-lactam antibiotics in aqueous solutions, International Journal of Pharmaceutics. 67 (1991) R5–R7. https://doi.org/10.1016/0378-5173(91)90438-T.
[15] C.-H. Liu, H.-Y. Huang, Antimicrobial Activity of Curcumin-Loaded Myristic Acid Microemulsions against Staphylococcus epidermidis, Chem. Pharm. Bull. 60 (2012) 1118–1124. https://doi.org/10.1248/cpb.c12-00220.
[16] G.B. Mahady, S.L. Pendland, G. Yun, Z.Z. Lu, Turmeric (Curcuma longa) and curcumin inhibit the growth of Helicobacter pylori, a group 1 carcinogen, Anticancer Res. 22 (2002) 4179–4181.
[17] R.C. Reddy, P.G. Vatsala, V.G. Keshamouni, G. Padmanaban, P.N. Rangarajan, Curcumin for malaria therapy, Biochemical and Biophysical Research Communications. 326 (2005) 472–474. https://doi.org/10.1016/j.bbrc.2004.11.051.
[18] L. Wright, J. Frye, B. Gorti, B. Timmermann, J. Funk, Bioactivity of Turmeric-derived Curcuminoids and Related Metabolites in Breast Cancer, CPD. 19 (2013) 6218–6225. https://doi.org/10.2174/1381612811319340013.
[19] K.T. Schmidt, W.D. Figg, The potential role of curcumin in prostate cancer: the importance of optimizing pharmacokinetics in clinical studies, Transl. Cancer Res. 5 (2016) S1107–S1110. https://doi.org/10.21037/tcr.2016.11.04.
[20] B.L. Tan, M.E. Norhaizan, Curcumin Combination Chemotherapy: The Implication and Efficacy in Cancer, (2019) 21.
[21] R.L. Edwards, P.B. Luis, P.V. Varuzza, A.I. Joseph, S.H. Presley, R. Chaturvedi, C. Schneider, The anti-inflammatory activity of curcumin is mediated by its oxidative metabolites, Journal of Biological Chemistry. 292 (2017) 21243–21252. https://doi.org/10.1074/jbc.RA117.000123.
[22] V. Kant, A. Gopal, N.N. Pathak, P. Kumar, S.K. Tandan, D. Kumar, Antioxidant and anti-inflammatory potential of curcumin accelerated the cutaneous wound healing in streptozotocin-induced diabetic rats, International Immunopharmacology. 20 (2014) 322–330. https://doi.org/10.1016/j.intimp.2014.03.009.
[23] Y. Henrotin, A.L. Clutterbuck, D. Allaway, E.M. Lodwig, P. Harris, M. Mathy-Hartert, M. Shakibaei, A. Mobasheri, Biological actions of curcumin on articular chondrocytes, Osteoarthritis and Cartilage. 18 (2010) 141–149. https://doi.org/10.1016/j.joca.2009.10.002.

[24] A.L. Lopresti, The Problem of Curcumin and Its Bioavailability: Could Its Gastrointestinal Influence Contribute to Its Overall Health-Enhancing Effects?, Advances in Nutrition. 9 (2018) 41–50. https://doi.org/10.1093/advances/nmx011.
[25] S. Peng, Z. Li, L. Zou, W. Liu, C. Liu, D.J. McClements, Improving curcumin solubility and bioavailability by encapsulation in saponin-coated curcumin nanoparticles prepared using a simple pH-driven loading method, Food Funct. 9 (2018) 1829–1839. https://doi.org/10.1039/C7FO01814B.
[26] W.-H. Tsai, K.-H. Yu, Y.-C. Huang, C.-I. Lee, EGFR-targeted photodynamic therapy by curcumin-encapsulated chitosan/TPP nanoparticles, IJN. Volume 13 (2018) 903–916. https://doi.org/10.2147/IJN.S148305.
[27] C. Tan, J. Xie, X. Zhang, J. Cai, S. Xia, Polysaccharide-based nanoparticles by chitosan and gum arabic polyelectrolyte complexation as carriers for curcumin, Food Hydrocolloids. 57 (2016) 236–245. https://doi.org/10.1016/j.foodhyd.2016.01.021.
[28] V. Kant, A. Gopal, D. Kumar, N.N. Pathak, M. Ram, B.L. Jangir, S.K. Tandan, D. Kumar, Curcumin-induced angiogenesis hastens wound healing in diabetic rats, Journal of Surgical Research. 193 (2015) 978–988. https://doi.org/10.1016/j.jss.2014.10.019.
[29] D.K. Kim, J. In Kim, B.R. Sim, G. Khang, Bioengineered porous composite curcumin/silk scaffolds for cartilage regeneration, Materials Science and Engineering: C. 78 (2017) 571–578. https://doi.org/10.1016/j.msec.2017.02.067.
[30] S.M. Andrabi, S. Majumder, K.C. Gupta, A. Kumar, Dextran based amphiphilic nano-hybrid hydrogel system incorporated with curcumin and cerium oxide nanoparticles for wound healing, Colloids and Surfaces B: Biointerfaces. 195 (2020) 111263. https://doi.org/10.1016/j.colsurfb.2020.111263.
[31] J. Liu, Z. Chen, J. Wang, R. Li, T. Li, M. Chang, F. Yan, Y. Wang, Encapsulation of Curcumin Nanoparticles with MMP9-Responsive and Thermos-Sensitive Hydrogel Improves Diabetic Wound Healing, ACS Appl. Mater. Interfaces. 10 (2018) 16315–16326. https://doi.org/10.1021/acsami.8b03868.
[32] F. Colucci, V. Mancini, C. Mattu, M. Boffito, Designing Multifunctional Devices for Regenerative Pharmacology Based on 3D Scaffolds, Drug-Loaded Nanoparticles, and Thermosensitive Hydrogels: A Proof-of-Concept Study, Pharmaceutics. 13 (2021) 464. https://doi.org/10.3390/pharmaceutics13040464.
[33] M.A. Tomren, M. Másson, T. Loftsson, H.H. Tønnesen, Studies on curcumin and curcuminoids, International Journal of Pharmaceutics. 338 (2007) 27–34. https://doi.org/10.1016/j.ijpharm.2007.01.013.
[34] P.R.K. Mohan, G. Sreelakshmi, C.V. Muraleedharan, R. Joseph, Water soluble complexes of curcumin with cyclodextrins: Characterization by FT-Raman spectroscopy, Vibrational Spectroscopy. 62 (2012) 77–84. https://doi.org/10.1016/j.vibspec.2012.05.002.
[35] R. Singh, H.H. Tønnesen, S.B. Vogensen, T. Loftsson, M. Másson, Studies of curcumin and curcuminoids. XXXVI. The stoichiometry and complexation constants of cyclodextrin complexes as determined by the phase-solubility method and UV–Vis titration, J Incl Phenom Macrocycl Chem. 66 (2010) 335–348. https://doi.org/10.1007/s10847-009-9651-5.
[36] H.H. Tønnesen, M. Másson, T. Loftsson, Studies of curcumin and curcuminoids. XXVII. Cyclodextrin complexation: solubility, chemical and photochemical stability, International Journal of Pharmaceutics. 244 (2002) 127–135. https://doi.org/10.1016/S0378-5173(02)00323-X.

[37] S. Khan, M.U. Minhas, M. Ahmad, M. Sohail, Self-assembled supramolecular thermoreversible β-cyclodextrin/ethylene glycol injectable hydrogels with difunctional Pluronic ® 127 as controlled delivery depot of curcumin. Development, characterization and *in vitro* evaluation, Journal of Biomaterials Science, Polymer Edition. 29 (2018) 1–34. https://doi.org/10.1080/09205063.2017.1396707.
[38] A. Ryzhakov, T. Do Thi, J. Stappaerts, L. Bertoletti, K. Kimpe, A.R. Sá Couto, P. Saokham, G. Van den Mooter, P. Augustijns, G.W. Somsen, S. Kurkov, S. Inghelbrecht, A. Arien, M.I. Jimidar, K. Schrijnemakers, T. Loftsson, Self-Assembly of Cyclodextrins and Their Complexes in Aqueous Solutions, Journal of Pharmaceutical Sciences. 105 (2016) 2556–2569. https://doi.org/10.1016/j.xphs.2016.01.019.
[39] B. Jana, S. Mohapatra, P. Mondal, S. Barman, K. Pradhan, A. Saha, S. Ghosh, α-Cyclodextrin Interacts Close to Vinblastine Site of Tubulin and Delivers Curcumin Preferentially to the Tubulin Surface of Cancer Cell, ACS Appl. Mater. Interfaces. 8 (2016) 13793–13803. https://doi.org/10.1021/acsami.6b03474.
[40] A.P. Gerola, D.C. Silva, S. Jesus, R.A. Carvalho, A.F. Rubira, E.C. Muniz, O. Borges, A.J.M. Valente, Synthesis and controlled curcumin supramolecular complex release from pH-sensitive modified gum-arabic-based hydrogels, RSC Adv. 5 (2015) 94519–94533. https://doi.org/10.1039/C5RA14331D.
[41] N.M. Patro, A. Sultana, K. Terao, D. Nakata, A. Jo, A. Urano, Y. Ishida, R.N. Gorantla, V. Pandit, K. Devi, S. Rohit, B.K. Grewal, E.M. Sophia, A. Suresh, V.K. Ekbote, S. Suresh, Comparison and correlation of in vitro, in vivo and in silico evaluations of alpha, beta and gamma cyclodextrin complexes of curcumin, J Incl Phenom Macrocycl Chem. 78 (2014) 471–483. https://doi.org/10.1007/s10847-013-0322-1.
[42] J. Hoque, N. Sangaj, S. Varghese, Stimuli-Responsive Supramolecular Hydrogels and Their Applications in Regenerative Medicine, Macromol. Biosci. 19 (2019) 1800259. https://doi.org/10.1002/mabi.201800259.
[43] Y. Okumura, K. Ito, R. Hayakawa, Theory on inclusion behavior between cyclodextrin molecules and linear polymer chains in solutions, Polym. Adv. Technol. (2000) 5.
[44] S. Loethen, J.-M. Kim, D.H. Thompson, Biomedical Applications of Cyclodextrin Based Polyrotaxanes, Polymer Revs. 47 (2007) 383–418. https://doi.org/10.1080/15583720701455145.
[45] A. Harada, J. Li, M. Kamachi, Preparation and properties of inclusion complexes of polyethylene glycol with .alpha.-cyclodextrin, Macromolecules. 26 (1993) 5698–5703. https://doi.org/10.1021/ma00073a026.
[46] T. Dong, Y. He, B. Zhu, K.-M. Shin, Y. Inoue, Nucleation Mechanism of α-Cyclodextrin-Enhanced Crystallization of Some Semicrystalline Aliphatic Polymers, Macromolecules. 38 (2005) 7736–7744. https://doi.org/10.1021/ma050826r.
[47] J. Li, A. Harada, M. Kamachi, Sol–Gel Transition during Inclusion Complex Formation between α-Cyclodextrin and High Molecular Weight Poly(ethylene glycol)s in Aqueous Solution, Polym J. 26 (1994) 1019–1026. https://doi.org/10.1295/polymj.26.1019.
[48] J. Li, X. Ni, K.W. Leong, Injectable drug-delivery systems based on supramolecular hydrogels formed by poly(ethylene oxide)s and ?-cyclodextrin, J. Biomed. Mater. Res. 65A (2003) 196–202. https://doi.org/10.1002/jbm.a.10444.
[49] J. Li, X. Li, Z. Zhou, X. Ni, K.W. Leong, Formation of Supramolecular Hydrogels Induced by Inclusion Complexation between Pluronics and α-Cyclodextrin, Macromolecules. 34 (2001) 7236–7237. https://doi.org/10.1021/ma010742s.

[50] G.G. Gaitano, W. Brown, G. Tardajos, Inclusion Complexes between Cyclodextrins and Triblock Copolymers in Aqueous Solution: A Dynamic and Static Light-Scattering Study, J. Phys. Chem. B. 101 (1997) 710–719. https://doi.org/10.1021/jp961996w.
[51] J. Li, X. Li, X. Ni, K.W. Leong, Synthesis and Characterization of New Biodegradable Amphiphilic Poly(ethylene oxide)- *b* -poly[(*R*)-3-hydroxy butyrate]- *b* -poly(ethylene oxide) Triblock Copolymers, Macromolecules. 36 (2003) 2661–2667. https://doi.org/10.1021/ma025725x.
[52] T. Higashi, A. Tajima, N. Ohshita, T. Hirotsu, I.I.A. Hashim, K. Motoyama, S. Koyama, R. Iibuchi, S. Mieda, K. Handa, T. Kimoto, H. Arima, Design and Evaluation of the Highly Concentrated Human IgG Formulation Using Cyclodextrin Polypseudorotaxane Hydrogels, AAPS PharmSciTech. 16 (2015) 1290–1298. https://doi.org/10.1208/s12249-015-0309-x.
[53] S.M.N. Simões, F. Veiga, J.J. Torres-Labandeira, A.C.F. Ribeiro, M.I. Sandez-Macho, A. Concheiro, C. Alvarez-Lorenzo, Syringeable Pluronic–α-cyclodextrin supramolecular gels for sustained delivery of vancomycin, European Journal of Pharmaceutics and Biopharmaceutics. 80 (2012) 103–112. https://doi.org/10.1016/j.ejpb.2011.09.017.
[54] A.J. Poudel, F. He, L. Huang, L. Xiao, G. Yang, Supramolecular hydrogels based on poly (ethylene glycol)-poly (lactic acid) block copolymer micelles and α-cyclodextrin for potential injectable drug delivery system, Carbohydrate Polymers. 194 (2018) 69–79. https://doi.org/10.1016/j.carbpol.2018.04.035.
[55] A. Abdul Karim, P.L. Chee, M.F. Chan, X.J. Loh, Micellized α-Cyclodextrin-Based Supramolecular Hydrogel Exhibiting pH-Responsive Sustained Release and Corresponding Oscillatory Shear Behavior Analysis, ACS Biomater. Sci. Eng. 2 (2016) 2185–2195. https://doi.org/10.1021/acsbiomaterials.6b00383.
[56] E. Khodaverdi, M. Aboumaashzadeh, F.S.M. Tekie, F. Hadizadeh, S.A.S. Tabassi, S.A. Mohajeri, Z. Khashyarmanesh, H.M. Haghighi, Sustained drug release using supramolecular hydrogels composed of cyclodextrin inclusion complexes with PCL/PEG multiple block copolymers, Iran Polym J. 23 (2014) 707–716. https://doi.org/10.1007/s13726-014-0265-4.
[57] T. Wang, X.-J. Jiang, Q.-Z. Tang, X.-Y. Li, T. Lin, D.-Q. Wu, X.-Z. Zhang, E. Okello, Bone marrow stem cells implantation with alpha-cyclodextrin/MPEG-PCL-MPEG hydrogel improves cardiac function after myocardial infarction, Acta Biomater. 5 (2009) 2939–2944. https://doi.org/10.1016/j.actbio.2009.04.040.
[58] J. Li, X. Li, X. Ni, X. Wang, H. Li, K.W. Leong, Self-assembled supramolecular hydrogels formed by biodegradable PEO–PHB–PEO triblock copolymers and α-cyclodextrin for controlled drug delivery, Biomaterials. 27 (2006) 4132–4140. https://doi.org/10.1016/j.biomaterials.2006.03.025.
[59] A. Domiński, T. Konieczny, P. Kurcok, α-Cyclodextrin-Based Polypseudorotaxane Hydrogels, Materials. 13 (2019) 133. https://doi.org/10.3390/ma13010133.
[60] Z. Li, H. Yin, Z. Zhang, K.L. Liu, J. Li, Supramolecular Anchoring of DNA Polyplexes in Cyclodextrin-Based Polypseudorotaxane Hydrogels for Sustained Gene Delivery, Biomacromolecules. 13 (2012) 3162–3172. https://doi.org/10.1021/bm300936x.
[61] C. Di Donato, R. Iacovino, C. Isernia, G. Malgieri, A. Varela-Garcia, A. Concheiro, C. Alvarez-Lorenzo, Polypseudorotaxanes of Pluronic® F127 with Combinations of α- and β-Cyclodextrins for Topical Formulation of Acyclovir, Nanomaterials. 10 (2020) 613. https://doi.org/10.3390/nano10040613.

[62] O.A. Budkina, T.V. Demina, T.Yu. Dorodnykh, N.S. Melik-Nubarov, I.D. Grozdova, Cytotoxicity of nonionic amphiphilic copolymers, Polym. Sci. Ser. A. 54 (2012) 707–717. https://doi.org/10.1134/S0965545X12080020.
[63] A. Torchio, M. Boffito, A. Gallina, M. Lavella, C. Cassino, G. Ciardelli, Supramolecular hydrogels based on custom-made poly(ether urethane)s and cyclodextrins as potential drug delivery vehicles: design and characterization, J. Mater. Chem. B. 8 (2020) 7696–7712. https://doi.org/10.1039/D0TB01261K.
[64] R. Laurano, C. Cassino, G. Ciardelli, V. Chiono, M. Boffito, Polyurethane-based thiomers: A new multifunctional copolymer platform for biomedical applications, Reactive and Functional Polymers. 146 (2020) 104413. https://doi.org/10.1016/j.reactfunctpolym.2019.104413.
[65] M. Boffito, A. Torchio, C. Tonda-Turo, R. Laurano, M. Gisbert-Garzarán, J.C. Berkmann, C. Cassino, M. Manzano, G.N. Duda, M. Vallet-Regí, K. Schmidt-Bleek, G. Ciardelli, Hybrid Injectable Sol-Gel Systems Based on Thermo-Sensitive Polyurethane Hydrogels Carrying pH-Sensitive Mesoporous Silica Nanoparticles for the Controlled and Triggered Release of Therapeutic Agents, Front. Bioeng. Biotechnol. 8 (2020) 384. https://doi.org/10.3389/fbioe.2020.00384.
[66] M. Boffito, E. Gioffredi, V. Chiono, S. Calzone, E. Ranzato, S. Martinotti, G. Ciardelli, Novel polyurethane-based thermosensitive hydrogels as drug release and tissue engineering platforms: design and *in vitro* characterization: Polyurethane-based thermosensitive hydrogels, Polym. Int. 65 (2016) 756–769. https://doi.org/10.1002/pi.5080.
[67] C. Pontremoli, M. Boffito, S. Fiorilli, R. Laurano, A. Torchio, A. Bari, C. Tonda-Turo, G. Ciardelli, C. Vitale-Brovarone, Hybrid injectable platforms for the in situ delivery of therapeutic ions from mesoporous glasses, Chemical Engineering Journal. 340 (2018) 103–113. https://doi.org/10.1016/j.cej.2018.01.073.
[68] R. Laurano, M. Boffito, A. Torchio, C. Cassino, V. Chiono, G. Ciardelli, Plasma Treatment of Polymer Powder as an Effective Tool to Functionalize Polymers: Case Study Application on an Amphiphilic Polyurethane, Polymers. 11 (2019) 2109. https://doi.org/10.3390/polym11122109.
[69] M. Wright, K. Kurumada, B. Robinson, Rates of incorporation of small molecules into pluronic micelles, in: M. Miguel, H.D. Burrows (Eds.), Trends in Colloid and Interface Science XVI, Springer Berlin Heidelberg, Berlin, Heidelberg, 2004: pp. 8–11. https://doi.org/10.1007/978-3-540-36462-7_3.
[70] X.J. Loh, L.W.I. Cheng, J. Li, Micellization and Thermogelation of Poly(ether urethane)s Comprising Poly(ethylene glycol) and Poly(propylene glycol), Macromol. Symp. 296 (2010) 161–169. https://doi.org/10.1002/masy.201051024.
[71] C. Schneider, O.N. Gordon, R.L. Edwards, P.B. Luis, Degradation of Curcumin: From Mechanism to Biological Implications, J. Agric. Food Chem. 63 (2015) 7606–7614. https://doi.org/10.1021/acs.jafc.5b00244.
[72] M. Heger, R.F. van Golen, M. Broekgaarden, M.C. Michel, The Molecular Basis for the Pharmacokinetics and Pharmacodynamics of Curcumin and Its Metabolites in Relation to Cancer, Pharmacol Rev. 66 (2014) 222–307. https://doi.org/10.1124/pr.110.004044.
[73] Mathematical models of drug release, in: Strategies to Modify the Drug Release from Pharmaceutical Systems, Elsevier, 2015: pp. 63–86. https://doi.org/10.1016/B978-0-08-100092-2.00005-9.

[74] B. Trathnigg, Size-Exclusion Chromatography of Polymers, in: R.A. Meyers (Ed.), Encyclopedia of Analytical Chemistry, John Wiley & Sons, Ltd, Chichester, UK, 2006: p. a2032. https://doi.org/10.1002/9780470027318.a2032.
[75] S. Caddeo, M. Mattioli-Belmonte, C. Cassino, N. Barbani, M. Dicarlo, P. Gentile, F. Baino, S. Sartori, C. Vitale-Brovarone, G. Ciardelli, Newly-designed collagen/polyurethane bioartificial blend as coating on bioactive glass-ceramics for bone tissue engineering applications, Materials Science and Engineering: C. 96 (2019) 218–233. https://doi.org/10.1016/j.msec.2018.11.012.
[76] X. Pang, Y. Jiang, Q. Xiao, A.W. Leung, H. Hua, C. Xu, pH-responsive polymer–drug conjugates: Design and progress, Journal of Controlled Release. 222 (2016) 116–129. https://doi.org/10.1016/j.jconrel.2015.12.024.
[77] C. Li, H. Li, Q. Wang, M. Zhou, M. Li, T. Gong, Z. Zhang, X. Sun, pH-sensitive polymeric micelles for targeted delivery to inflamed joints, Journal of Controlled Release. 246 (2017) 133–141. https://doi.org/10.1016/j.jconrel.2016.12.027.
[78] J. Liu, Y. Huang, A. Kumar, A. Tan, S. Jin, A. Mozhi, X.-J. Liang, pH-Sensitive nano-systems for drug delivery in cancer therapy, Biotechnology Advances. 32 (2014) 693–710. https://doi.org/10.1016/j.biotechadv.2013.11.009.
[79] C. Pradal, K.S. Jack, L. Grøndahl, J.J. Cooper-White., Gelation Kinetics and Viscoelastic Properties of Pluronic and α-Cyclodextrin-Based Pseudopolyrotaxane Hydrogels, Biomacromolecules. 14 (2013) 3780–3792. https://doi.org/10.1021/bm401168h.
[80] R. Sadeghi, F. Jahani, Salting-In and Salting-Out of Water-Soluble Polymers in Aqueous Salt Solutions, J. Phys. Chem. B. 116 (2012) 5234–5241. https://doi.org/10.1021/jp300665b.
[81] B.C. Anderson, S.M. Cox, A.V. Ambardekar, S.K. Mallapragada, The effect of salts on the micellization temperature of aqueous poly(ethylene oxide)-b-poly(propylene oxide)-b-poly(ethylene oxide) solutions and the dissolution rate and water diffusion coefficient in their corresponding gels, Journal of Pharmaceutical Sciences. 91 (2002) 180–188. https://doi.org/10.1002/jps.10037.
[82] J.W. Chung, T.J. Kang, S.-Y. Kwak, Supramolecular Self-Assembly of Architecturally Variant α-Cyclodextrin Inclusion Complexes as Building Blocks of Hexagonally Aligned Microfibrils, Macromolecules. 40 (2007) 4225–4234. https://doi.org/10.1021/ma0625105.
[83] L. Huang, E. Allen, A.E. Tonelli, Study of the inclusion compounds formed between α-cyclodextrin and high molecular weight poly(ethylene oxide) and poly(ϵ-caprolactone), Polymer. 39 (1998) 4857–4865. https://doi.org/10.1016/S0032-3861(97)00568-5.
[84] U. Ahmad, M. Sohail, M. Ahmad, M.U. Minhas, S. Khan, Z. Hussain, M. Kousar, S. Mohsin, M. Abbasi, S.A. Shah, H. Rashid, Chitosan based thermosensitive injectable hydrogels for controlled delivery of loxoprofen: development, characterization and in-vivo evaluation, International Journal of Biological Macromolecules. 129 (2019) 233–245. https://doi.org/10.1016/j.ijbiomac.2019.02.031.
[85] B. Jeong, Y.H. Bae, S.W. Kim, Thermoreversible Gelation of PEG−PLGA−PEG Triblock Copolymer Aqueous Solutions, Macromolecules. 32 (1999) 7064–7069. https://doi.org/10.1021/ma9908999.
[86] W. Brown, K. Schillen, S. Hvidt, Triblock copolymers in aqueous solution studied by static and dynamic light scattering and oscillatory shear measurements: influence of relative block sizes, J. Phys. Chem. 96 (1992) 6038–6044. https://doi.org/10.1021/j100193a072.
[87] C.L. McCormick, ed., Stimuli-Responsive Water Soluble and Amphiphilic Polymers, American Chemical Society, Washington, DC, 2000. https://doi.org/10.1021/bk-2001-0780.

[88] X. Song, Z. Zhang, J. Zhu, Y. Wen, F. Zhao, L. Lei, N. Phan-Thien, B.C. Khoo, J. Li, Thermoresponsive Hydrogel Induced by Dual Supramolecular Assemblies and Its Controlled Release Property for Enhanced Anticancer Drug Delivery, Biomacromolecules. 21 (2020) 1516–1527. https://doi.org/10.1021/acs.biomac.0c00077.
[89] E. Segredo-Morales, M. Martin-Pastor, A. Salas, C. Évora, A. Concheiro, C. Alvarez-Lorenzo, A. Delgado, Mobility of Water and Polymer Species and Rheological Properties of Supramolecular Polypseudorotaxane Gels Suitable for Bone Regeneration, Bioconjugate Chem. 29 (2018) 503–516. https://doi.org/10.1021/acs.bioconjchem.7b00823.
[90] S. Seçer, D. Ceylan Tuncaboylu, Supramolecular poloxamer-based *in situ* gels with hyaluronic acid and cyclodextrins, International Journal of Polymeric Materials and Polymeric Biomaterials. (2021) 1–9. https://doi.org/10.1080/00914037.2021.1876055.
[91] L. Tong, Y. Yang, X. Luan, J. Shen, X. Xin, Supramolecular hydrogels facilitated by α-cyclodextrin and silicone surfactants and their use for drug release, Colloids and Surfaces A: Physicochemical and Engineering Aspects. 522 (2017) 470–476. https://doi.org/10.1016/j.colsurfa.2017.03.026.
[92] S. Hewlings, D. Kalman, Curcumin: A Review of Its Effects on Human Health, Foods. 6 (2017) 92. https://doi.org/10.3390/foods6100092.
[93] S. Xu, L. Yin, Y. Xiang, H. Deng, L. Deng, H. Fan, H. Tang, J. Zhang, A. Dong, Supramolecular Hydrogel from Nanoparticles and Cyclodextrins for Local and Sustained Nanoparticle Delivery, Macromol. Biosci. 16 (2016) 1188–1199. https://doi.org/10.1002/mabi.201600076.
[94] X. Yao, J. Mu, L. Zeng, J. Lin, Z. Nie, X. Jiang, P. Huang, Stimuli-responsive cyclodextrin-based nanoplatforms for cancer treatment and theranostics, Mater. Horiz. 6 (2019) 846–870. https://doi.org/10.1039/C9MH00166B.